Imperial College London

Department of Electrical and Electronic Engineering

Final Year Project Report 2013

| | |
|---|---|
| Project Title: | **Intelligent Solar Charge Controller for Domestic Off-grid Solar Systems** |
| Student: | **A. Grealish** |
| CID: | **00597408** |
| Course: | **4T** |
| Project Supervisor: | **Professor A. Holmes** |
| Second Marker: | **Professor R. Syms** |

*I would like to thank all of the e.quinox team, especially Christopher Emmott and Yuval Jacob who worked with me during the 2012 trial of e.quinox's izuba.box and Matthew Wood who has helped with mechanical designs and sourcing of the enclosure. I would also like to thank Engineers Without Borders UK for supporting this project through affiliation and helping to promote it to the wider development community and Appropriate Technology magazine for writing an article on this project.*

*The IET, ARM and Total have kindly all contributed financially to this project. Total deserves many thanks for their contribution which was used for financing the 2012 trial. ARM and the IET deserve equal thanks for their contributions which are being used to fund the development and deployment of the 2013 trial.*

*Final thanks go to Professor Andrew Holmes for kindly supervising this project.*



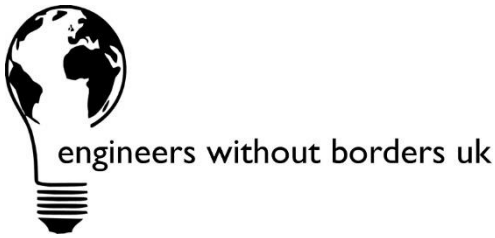




# Abstract

There are 1.4 billion people worldwide living without access to electricity. Providing these people with access to electricity can have a huge impact on their income, education and health. Across Africa people are using Kerosene for lighting which produces poor quality light but more importantly releases toxic fumes and can easily cause severe burns. The movement to eradicate Kerosene is growing but there are still many barriers for the end customers, one of the biggest being the lack of finance for purchasing alternatives.

One alternative is the Solar Home System; this is typically a PV (solar) panel, storage battery and LED lights. These are selling in large numbers to the richer consumers in developing nations but are still too expensive for consumers at the bottom of the income pyramid. In 2012 with e.quinox, I developed a prototype Solar Home System called the izuba.box that could be purchased on a pay-as-you-go plan. This meant that we could better replicate the business model of Kerosene, which is to sell small quantities frequently, making an expensive product more affordable to the end customer. The 2012 prototype was trialled in Rwanda and highlighted many areas for improvement, the most important being the poor quality charge controller which shortened battery lifetime.

The desired outcome of this project is an open-source but commercially viable izuba.box which integrates an intelligent charge controller. The charge controller is designed to extend the useable lifetime of the sealed lead-acid batteries whilst making the most efficient use of the PV panel. This will help to reduce the cost and environmental impact of the izuba.box and better meet its original aims of being a truly affordable alternative to Kerosene.

The charge controller has now been designed, tested and is ready for trial deployment. The charge controller makes use of a technique called interrupted charge control which was shown to increase battery lifetime by up to 400% when used with an unlimited power source. This gain in battery lifetime is mostly due to the reduction in overcharging which normally occurs during current charge control algorithms. The innovation in this project is applying interrupted charge control to small PV system with unreliable and intermittent power. This means that maximum power point tracking, temperature dependence and on-load battery charging must be considered to ensure that the system is optimised for battery lifetime without impacting the usability.

A secondary aim of the project is to reduce the manufacturing and assembly time and complexity of the product whilst increasing the reliability and robustness. The product is now designed as a single PCB which combines the charge controller, payment system and user interface. The PCBs and matching casings can easily be manufactured by external partners without specialist electronics or engineering knowledge. This was done so that organisations that are larger than e.quinox can use these designs for their own trials or even large scale distribution to start to tackle the electrification problem on a bigger scale.

There is still work to be done in this project. Long-term battery lifetime tests could not be completed in the timeframe and battery temperature based test proved inconclusive. However, the product is designed to include an optional data-logging unit which can be used by e.quinox to perform a full analysis following a trial of 100 units which will commence in Rwanda during the summer of 2013.

# TABLE OF CONTENTS

# Introduction

# Overview

This project aims to develop a charge controller suitable for use in domestic off-grid solar systems. The developed charge controller will be incorporated within a pay-as-you-go solar home system named the izuba.box which is designed to provide low income groups in developing nations with clean access to lighting and electricity. The project is affiliated with e.quinox, an Imperial College based, student run project, and Engineers Without Borders UK, an international development organisation. During the summer of 2013 the izuba.box will be manufactured and used in a trial of 100 households in Rwanda. This report discusses the motivations behind this project, background research and the final implementation. Importantly, it also highlights the future work required and lessons learnt.

## The Electrification Problem

There are 1.4 Billion people living worldwide without access to electricity (1). In Africa 57% of the population live without access and this is predicted to rise to 67% by 2030 (2). In Rwanda specifically only 7% have access (3) and in rural areas this falls to 1%. Bringing electricity and lighting to these areas can have a huge impact; productivity can increase as people work and do business later into the evening which boosts the local economy. School children can study later into the evenings allowing them to achieve better grades, and finally it reduces the travelling required to recharge mobile phones and to purchase Kerosene for lighting.

The passage below is a message received from a young person living in a small village in Northern Rwanda where e.quinox first trialled the izuba.box concept. It shows the impact that clean and easy access to electricity can have.

> *"I really like your project here ,it is quiet awesome to see my small quarter called MUNYANA(Minazi) at the evening all blight with the light provided by your organization e.quinox. previously, we were mainly based on petrol lights or candles for some people, but to day it is note the case due to equinox. moreover it was so hard to recharge our phones, you can imagine that the people did about 5 kilometers to get to the sector office to recharge their phones because it was there only found electricity along over the whole sector. but to day we almost use boxes to recharge." [sic]*

Many people would argue that a commercially viable solution cannot be used to solve the electrification problem as they believe target consumers do not have the money to support a for-profit venture. This however, is a misconception. The market currently spends $37 billion dollars on low quality energy solutions (4). Businesses need to change their models to enable profit to be generated from this new market.

Bottom of the pyramid (BOP) consumers cannot afford to pay large amounts of cash for a product and are much better served by small, frequent payments. For example, shampoo is often sold to these markets in single use sachets rather than large bottles allowing the price sensitive consumer to purchase just what they need for that day (5). A second example is how people are currently buying Kerosene, the fuel used for lighting. People purchase only enough to last a few days rather than buying in bulk which is potentially cheaper. By applying this business methodology to electrification, the issues can be tackled in a sustainable and large scale way by for-profit companies.

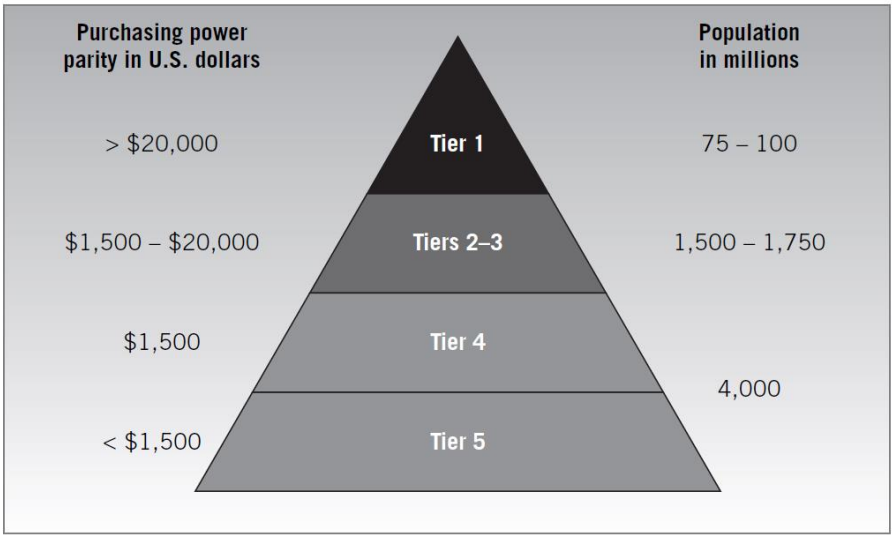


**Figure 1 - The Economist Pyramid showing the huge size of the market of Bottom of the Pyramid consumers. Whilst the consumers in tiers 4 & 5 have less purchasing power each there are many more of them making the market worthwhile targeting (5).**

## Current Solar Home Systems

Many companies are entering the developing nation's electrification market with products known as solar home systems (SHSs) or solar lanterns (SLs). These are solar powered systems, with storage batteries providing lighting and often mobile phone charging. Bboxx and DLight are examples of companies supplying these systems commercially.

**Figure 2 - Bboxx's BB5 Solar Home System and D.light's S250 Solar Lantern**

These are selling well to the richer consumers in developing nations and are often purchased in bulk by NGO's such as Solar Sister (6) to be given to the end customers. Through NGO's they can be distributed to the poorest customers who need them most but this is not a sustainable solution. A real solution is to provide a product which is affordable to even the bottom of the pyramid customers.

## E.QUINOX

e.quinox is a non-profit, student-led, humanitarian project that aims to bring cost-effective, sustainable and renewable energy to developing countries (7). e.quinox aims to prove that certain business models and technologies work thus encouraging the uptake of these models by larger

NGOs or for-profit organisations. The core belief of e.quinox is that the electrification problem can only be solved with financially viable business models rather than relying on aid.

Since 2009 e.quinox has been experimenting with an energy kiosk model and has built 6 energy kiosks across Rwanda and Tanzania. An energy kiosk is a small building at the centre of a village with a solar battery charging system which is used by a shopkeeper to charge battery boxes. A battery box is a sealed lead-acid battery with protection and power level conversion circuitry allowing it to power LED lighting and charge mobile phones. Customers rent a fully charged battery box, take it to their homes and return it when the battery is depleted.

However, during the trials of the energy kiosk model many issues have been identified, both technically and from a business perspective. One of the identified issues with the energy kiosk is that it is not suitable for very rural areas with a very sparse population density. It is designed to be placed in the centre of a village however we have found that people may walk for 5 km or more to rent a battery box (8). Another identified issue is one of bookkeeping and management. In each kiosk e.quinox employs a shopkeeper who is paid through the profits generated. They are in charge of keeping track of the finances and ensuring all customers have paid for their rentals. However due to the lack of education or occasionally corruption the shopkeepers do not correctly log this data. Whilst analysing performance of each kiosk e.quinox members often find the accounts to be so badly kept that the data is unusable.

## Preceding Work

During 2012 e.quinox experimented with a new solution for electrification of rural communities which improved upon some of the issues associated with the energy kiosk and solar home systems. I developed a prototype of the solution which was branded the izuba.box (izuba means solar in Kinyarwandan, the local language in Rwanda) which removes the requirement for a kiosk and extends the battery box to incorporate power generation facilities. Each izuba.box was supplied with its own solar panel, charge controller and payment system.

**Figure 3 – Prototype izuba.box which was Trialled in Rwanda in 2012.**

The izuba.box is similar to a Solar Home System but with the addition of an innovative business model. Customers are given the izuba.box on a pay-as-you-go, hire purchase scheme. Payment is made using a mobile phone based money transfer system which is already widely used in Rwanda and surrounding countries. Money is transferred to e.quinox from the customer and they receive a SMS reply with a unique unlock code for their system. The unlock code is typed into the keypad on the izuba.box which verifies the code and allows the user as much access as they have paid for.

The izuba.box concept has many advantages over the energy kiosk model. Firstly, the cost of building, maintaining and operating a central kiosk is removed. This removes the need for a shopkeeper to manage the bookkeeping as this is now all managed by on automated system which generates the unlock codes. However we will still employ an individual to manage the distribution and maintenance of the systems. The online interface to the payment system is shown in Figure 4. This is only ever accessed by e.quinox and its employees in Rwanda who manage the trial. Customers interact with the payment system solely though their mobile phones.

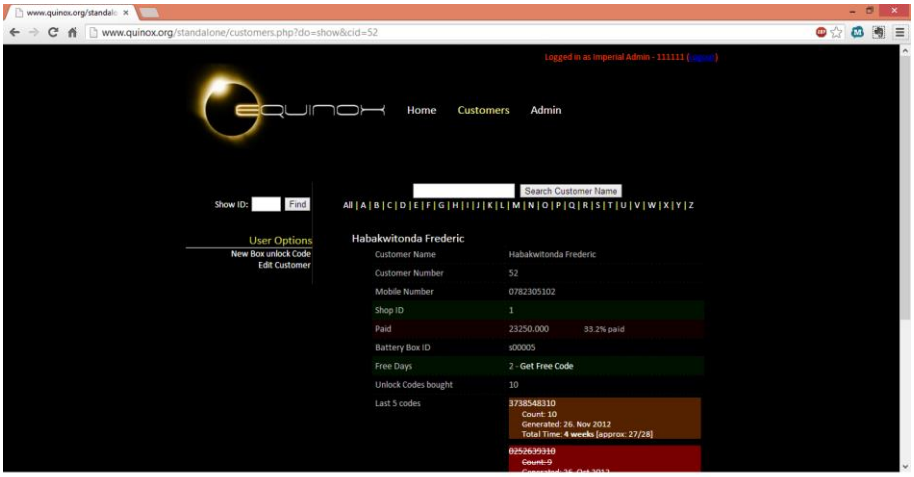


**FIGURE 4 - ONLINE PORTAL FOR CUSTOMER ACCOUNT MANAGEMENT AND UNLOCK CODE GENERATION. CUSTOMERS DO NOT ACCESS THIS PAGE, INSTEAD THEY AUTOMATICALLY RECEIVE THE UNLOCK CODES VIA SMS AFTER TRANSFERRING MONEY TO E.QUINOX THOUGH MOBILE MONEY TRANSFER SYSTEMS.**

One benefit to the customers is that the izuba.box costs a similar price to Bboxx's BB7 (Figure 2) however the addition of a pay-as-you-go payment business model and technical implementation of this makes the product affordable to almost all customers. The monthly price charged for a payback period of 2 years is less than the average bottom of the pyramid consumer is spending on low quality energy solutions currently.

A second customer benefit is that the box is charged and paid for in the user's home meaning that the time previously spend travelling to gain access to electricity is now freed. People may still need to travel to top up their mobile money credit, however the mobile phone networks already have very good distribution networks in place for this.

A trial of 75 prototype izuba.boxes (shown in Figure 3) were deployed in Rwanda's northern Provence in September 2012. They were distributed to a range of customer types but focusing on the bottom income group in the most rural areas. The test customers chosen were known to the shopkeeper at one of e.quinox's existing kiosks meaning we have easier access to the customers for feedback.

Many issues have been identified which need to be addressed before large scale deployment of this product. These issues have been identified through customer and shopkeeper feedback as well as by analysing data from the unlock code generation system (Figure 4) and through detailed reliability analysis of the current design. The first issue identified was the third party charge controller which was used within the boxes. The charge controller used is the most basic type, it connects the panel and battery directly together with a high voltage and low voltage disconnect. There are many implications of this which will be discussed in more detail in this report; the mains issues include reduced power available from the panel and shortened battery lifetime. Due to the reduction of battery lifetime e.quinox estimates that the batteries used in the first generation izuba.box will fail before the end of the payback period, for this reason we have covered the cost of a replacement battery in the total price of each unit.

Based on the feedback and knowledge gained from this trial the objectives for improvement and the basis for this project have been decided.

# Project Aims

The primary aim of this project is to incorporate an intelligent maximum power point tracking (MPPT) charge controller into the payment system and output conversion electronics allowing full utilisation of the solar panel and ensure a replacement battery is not required during the products lifetime. The integration of the payment system and charge controller is beneficial as many components are duplicated when separated. Both systems require a method for detecting battery charge and switching of the outputs when battery is low. By integrating these systems together we reduce costs and increase the intelligence of the overall system.

## Primary Aim

***Develop an intelligent, low cost maximum power point tracking charge controller and battery management system to extend battery lifetime.***

The above aim specifies 4 desired attributes for the designed charge controller:

- Intelligence: the charge controller should consider factors such as the health of the battery and the maximum amount of power available from the PV panel and carefully balance the battery charging algorithm to provide an optimal charging and discharging technique.
- Low cost: this product is targeted at low income consumers in developing nations, for this reason the product should be as low cost as possible without compromising on quality or reliability.
- Maximum power point tracking: the PV panel is a large part of the component cost of this product, for this reason the full power should be extracted from it when suitable.
- Battery lifetime extending: the battery is the largest single cost component in the product and is most likely to fail. For this reason the charge controller should prolong lifetime as much as possible.

Research has been published separately into the individual attributes of the goal but it is difficult to find research combining all aspects into a single charge controller. Intelligent, multi-stage charge controllers have been widely commercialised but are often very expensive. The same can be said for maximum power point tracking but this functionality is rarely combined with multi-stage charging. Charge controllers that extend battery lifetime are mostly mains powered, there are very few, if any, commercially available solar charge controllers with this functionality.

Most research published on charge controllers focus on large sealed lead-acid batteries, typically > 30Ahr. This is due to most research looking at uninterruptable power supplies for telecommunications systems, automotive applications or large photovoltaic systems. As this product is a photovoltaic systems for a single household the required batteries are much smaller, typically 7-10AHrs. Because of this many charge controllers designed in current research have much higher power ratings than is required here. The algorithms used to detect charge the batteries will need to be modified and optimised for these smaller systems.

## Secondary Aim

**Redesign the izuba.box to reduce manufacturing time whilst increasing durability and reliability.**

This secondary aim will involve combining the charge controller technology and the solar home system to make a full and commercially viable product which is reliable and easy to assemble. The

2012 prototype izuba.box suffered from reliability issues and took a very long time to manufacture. This is due to all the connectors being wired and connected to the PCB through terminal block as shown in Figure 5. One easy improvement to reduce assembly time is to mount all the connectors directly to the PCB and machine the faceplate to match. This should also increase the reliability of the product as failures due to repeated flexing of wires will be prevented.

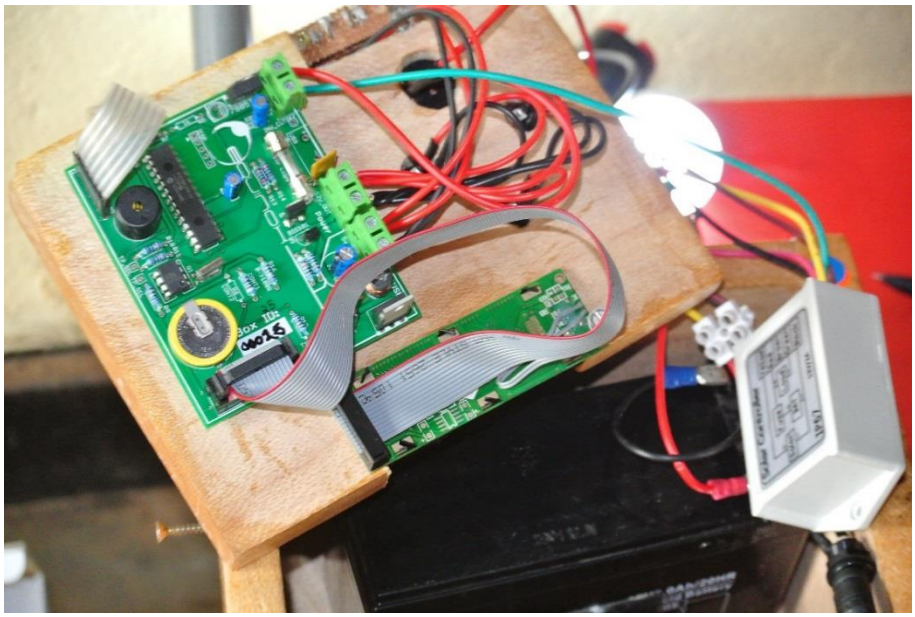

**FIGURE 5 - 2012 IZUBA.BOX PROTOTYPE. THIS DEMONSTRATES THE EXCESSIVE WIRING AND POOR CONNECTOR MOUNTING.**

A second motivation for this aim links back to e.quinox's strategy for tackling the electrification problem on a large scale. As a student-run organisation, e.quinox cannot itself have a huge impact but, if it proves that certain business models and technologies work then other organisations may adopt these solutions. If e.quinox relies on large amounts of free student labour in the assembly of these boxes then our trials are an unrealistic representation of what another organisation could replicate.

For these reasons this product will be designed with machine assembly in mind and we will be using partner companies to assemble the electronics and the faceplates. Final assembly of the units will still be completed in Rwanda with a potential customers being employed by e.quinox but as this required little technical knowledge we feel that this is easily replicable. e.quinox will pay for any tooling fees required for machine assembly meaning that in the future any companies wishing to replicate the solution can simply re-order the design from our partner companies.

# Background

# PV Panels

Solar systems have long exploited the benefits of PV panels to deliver power to rural off-grid areas of developing nations. This project will use a PV panel of poly-crystalline silicon cells, purchased from a third party. To analyse the magnitudes of power, voltage and current we must first understand the operating principles of a PV panel.

## PV Panel Operating Principles

PV Panels have three important parameters. These are:

- Peak power, $W_P$ – The power a panel will produce at 25°C under an irradiance of 1000 W/m$^2$ (9). While this parameter is specified at 25°C, many PV panel manufactures quote ratings at 45°C as this is more representative of normal operating conditions (10).
- Open Circuit Voltage, $V_{OC}$ – The voltage present across the terminals of the solar panel when open circuit. This sets the maximum operating voltage of a PV panel at 25°C, 1000 W/m$^2$.
- Short Circuit Current, $I_{SC}$ – The current through the solar cell when the voltage is zero. Again, this is measured at 25°C, 1000 W/m$^2$.

These parameters can be obtained from the IV plot of the panel as shown below:

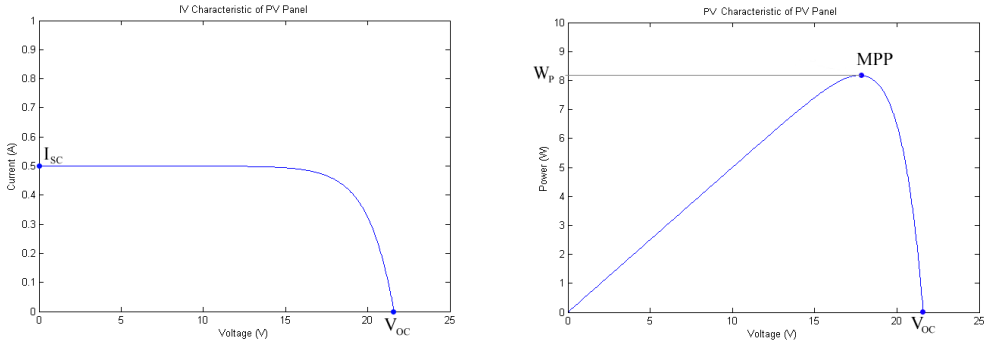


**Figure 6 - Current and Power Characteristics Against Voltage. For this Panel ISC=0.5A and VOC=22V. $W_P$=8.2W.**

## PV Panel Modelling

Two types of simulation are required for this project. The first simulation type is use to test charge control algorithms. Simulink is used for this as it allows hardware models to be combined with software scripts to test algorithms. Simulink includes a PV cell model which can be duplicated to create a model of a full PV panel.

The second simulation required is of the analogue electronics used in the DC-DC converter, for this LTSpice has been used. LTSpice does not contain a PV Panel model. The model was made with a diode model published online (11). The simulated characteristics of this model are shown in Figure 7.

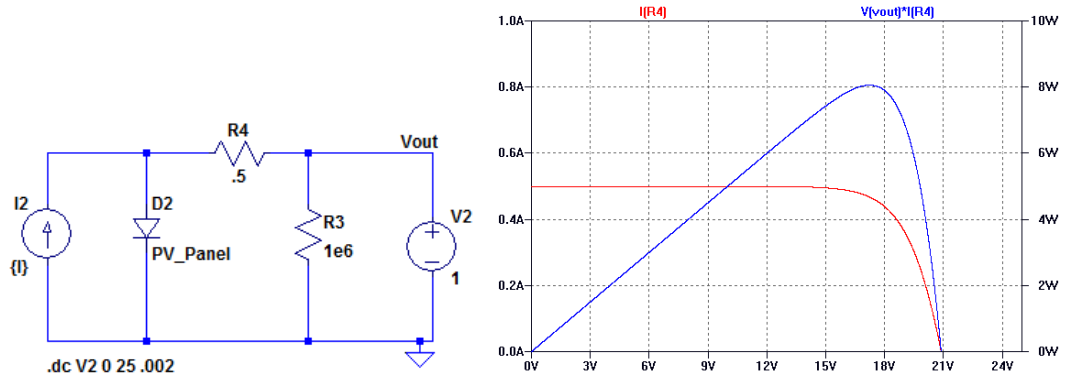


**Figure 7 - PV Panel Simulation in LTSpice. The graph show Current and Power against panel operating voltage**

## Maximum Power Point Tracking

The peak power in Figure 6 is labelled MPP (Maximum Power Point), MPP is a more general term for the maximum power that can be extracted from a solar panel under any level of irradiance and at any temperature. Figure 6 is plotted at 25°C and 1000W/m$^2$ the MPP is equal to the Peak power. Figure 8 shows the Power Voltage plot under a range of irradiance levels, the MPP moves as irradiance changes.

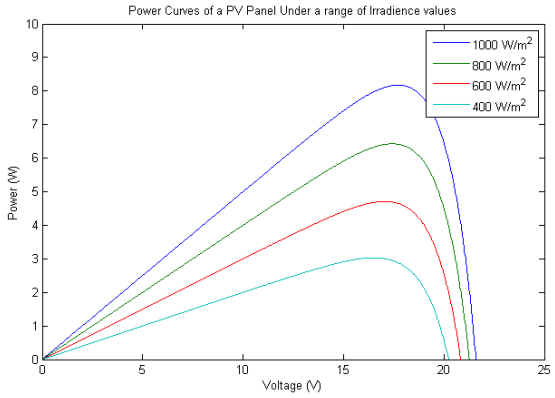


**Figure 8 - Power Curves of a PV Panel At a Range of Irradiance Levels.**

It is clear that the MPP will move during normal use due to daily variations in irradiance and cloud shadowing. To extract the most power from the panel at any given time the MPP must be tracked by adjusting the magnitude of the load attached to the panel. This is the main operating principle behind a Maximum Power Point Tracking (MPPT) Charge Controller which combines a DC-DC converter and software algorithms to adjust the load on the panel and thus the operating voltage.

One of the most commonly used algorithms is Perturb and Observe (12). The maximum power point will be tracked by perturbing the duty cycle and observing the change in power output. If the power output increases the direction of the perturbation is repeated, if power falls the direction is reversed. The typical control flow is shown in Figure 9.

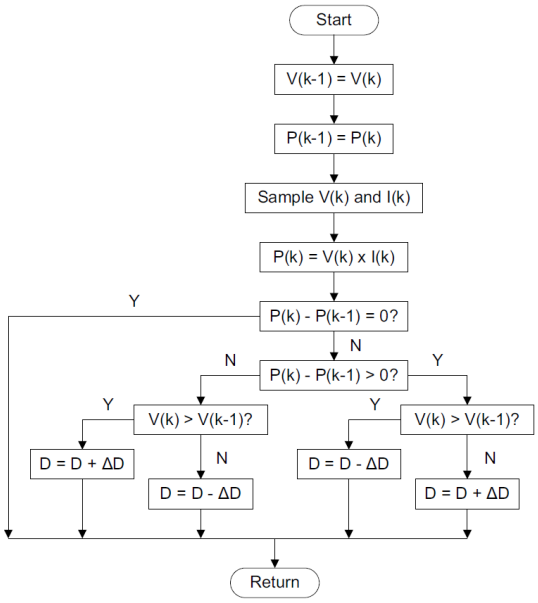


FIGURE 9 - CONTROL FLOW OF CONVENTIONAL P&O METHOD (13).

This algorithm has been implemented in a MatLab script and tested with the above Simulink model of the system. Figure 10 and Figure 11 show the results of the Simulink simulations. Both show the power being pulled from the panel on the left and the duty cycle of the switching MOSFET on the left.

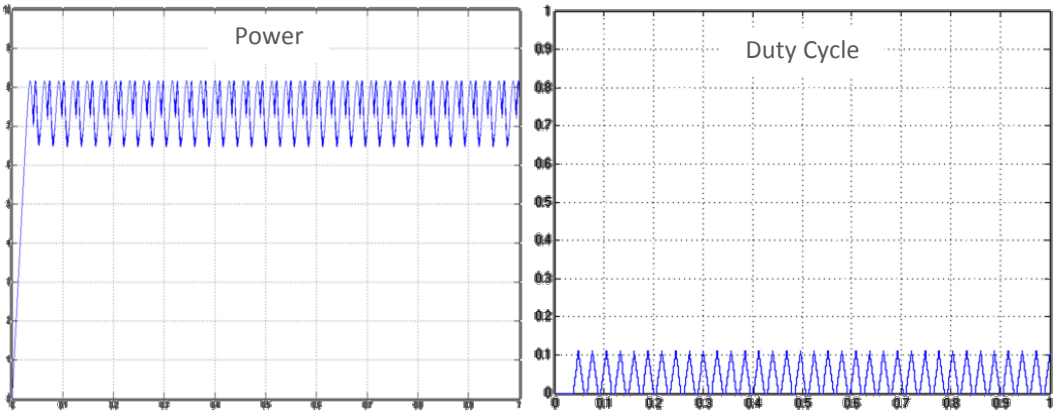


FIGURE 10 - SIMULATION OF THE MPPT CHARGE CONTROLLER WITH A LARGE DUTY CYCLE DELTA.

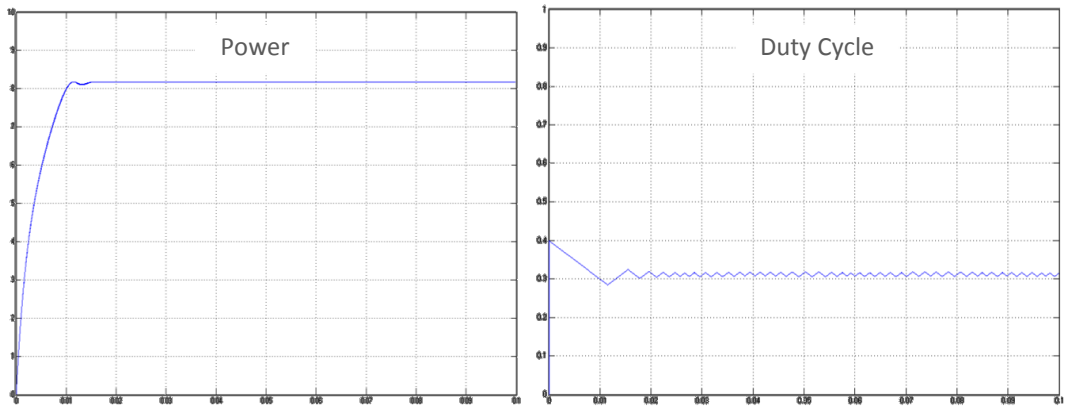


FIGURE 11 - SIMULATION OF THE MPPT CHARGE CONTROLLER WITH A SMALL DUTY CYCLE DELTA.

As we have seen in Figure 10 and Figure 11 the chosen duty cycle delta, the amount by which duty cycle is varied, affects the operation of the MPPT. A large duty cycle delta allows the algorithm to track changes in MPP quickly but a smaller duty cycle delta means smaller fluctuations around the MPP in constant irradiance situations. P&Ob is a modified version of the P&O algorithm, where a fixed duty cycle delta is not used, instead the delta is changed so that it reduces around the MPP and increases for quicker tracking in fast changing conditions.

P&O is a simple MPPT algorithm but many alternative algorithms have been proposed and evaluated in research papers. M. Berrera's experimental review of MPPT algorithms was studied (14). This paper compares classical P&O (P&Oa), modified P&O (P&Ob), three point weight comparison (P&Oc), Constant Voltage (CV), incremental conductance (IC), open circuit voltage (OV) and shortcurrent pulse (SC). The paper ran tests to compare the algorithms in terms of total energy output under two irradiance profiles shown in Figure 12.

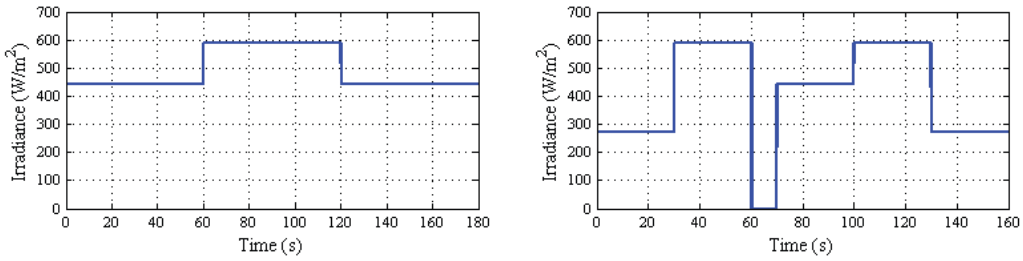


FIGURE 12 –THE IRRADIANCE PROFILES FOR THE TESTS, RESULTS SHOWN BELOW (14).

TABLE II.
ENERGY GENERATED AS A FUNCTION OF MPPT TECHNIQUE AND IRRADIANCE INPUT

| MPPT Technique | Case 1 Energy [J] | Case 1 Rank | Case 2 Energy [J] | Case 2 Rank |
|---|---|---|---|---|
| P&Oa | 4222 | 3 | 3119 | 2 |
| P&Ob | 4330 | 1 | 3197 | 1 |
| P&Oc | 4261 | 2 | 3104 | 3 |
| IC | 4175 | 4 | 3035 | 5 |
| CV | 4086 | 6 | 2984 | 6 |
| OV | 4145 | 5 | 3038 | 4 |
| SC | 4059 | 7 | 2970 | 7 |

FIGURE 13 - ENERGY GENERATED AS A FUNCTION OF MPPT TECHNIQUE AND IRRADIANCE INPUT (14).

The experimental results from this investigation into MPPT algorithms show that P&O based techniques provide the best results. P&Oc requires higher complexity than the P&Oa, so the extra

costs must be considered when choosing algorithm. OV and SC require making changes to a typically DC-DC converter making these techniques undesirable, especially considering their lower performance. P&Ob showed the best results in the tests but it's response in low irradiance levels may be slightly worse than other P&O techniques.

This evaluation compared the listed MPPT algorithms with a fixed duty-cycle variation, $\Delta\partial$ (except P&Ob which alters $\Delta\partial$ as part of the algorithm) and time interval. These two values can be further optimised for the expected usage environment. A reduced duty cycle variation allows the MPP to be found more accurately but slows down the tracking. This can be countered by reducing the time interval but this will increase the required computation power. These parameters must be optimised to get high performance in terms of efficiency and cost.

## Yearly Solar Insolation Data From Rwanda

Given solar panel parameters the total annual power in a certain region can be estimated given the Insolation (Energy per Area of PV Panel) data. The target area for this product is central Africa, more specifically Northern Rwanda which only has one reliable insolation measurement station at Kigali Airport (15). Geostationary satellites can give irradiance estimations over a course grid. Figure 15 shows yearly insolation data obtained using a variety of measurements techniques but shows a good estimate for yearly insolation in Rwanda. We see that for Northern Rwanda we can expect 2000 – 2100 kWh/m$^2$ over an average year.

Taking the 7 $W_P$ PV Panel used with the izuba.box as an example the would give a total panel output of 54 Wh per day. Assuming the system is 50% efficient at storing the PV energy this would give the user 38Wh of energy usage on an average day, this will equate to 5 hours of mobile phone charging and 13 hours of 2W LED bulb lighting. The 50% efficiency is a rough estimation of system efficiency and includes inefficiencies arising from sub-optimal PV panel placement, finite storage capacity, power losses in electronics and standby power consumption.

The above estimation is based on the assumption that the irradiance does not fluctuate due to seasonal variations. Figure 14 estimates the seasonal variations using three models. This shows that seasonal variation is only 10% which will not have a large impact on the user as the system is deliberately oversized to counter this. This would be important for countries further from the equator.

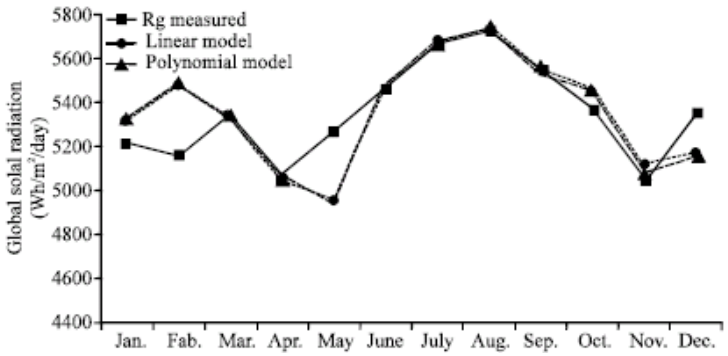


**Figure 14 – Seasonal variations in irradiance for Kigali Airport, Rwanda (15).**

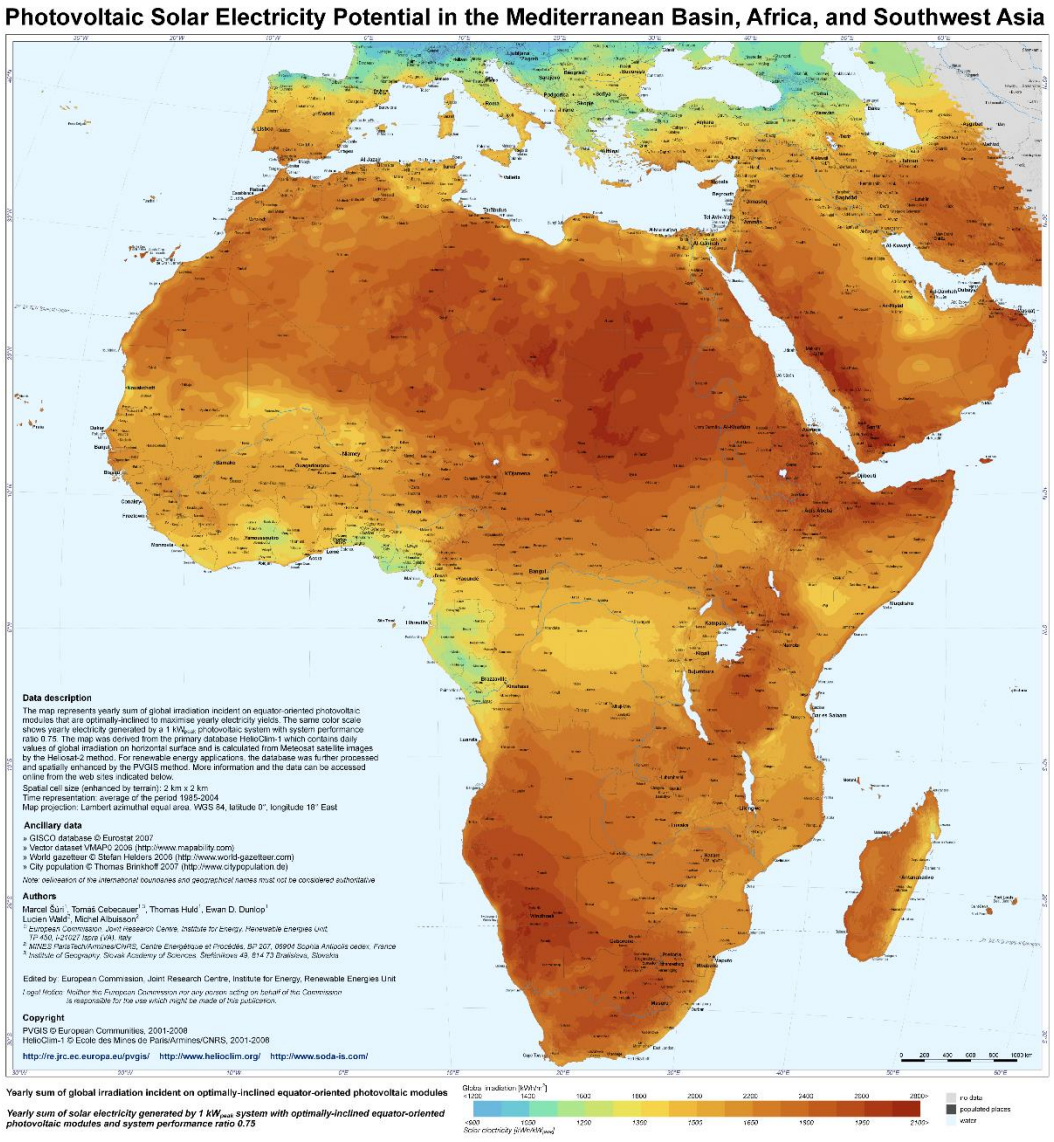


**FIGURE 15 – MAP SHOWING ANNUAL SUM OF IRRADIANCE ACROSS AFRICA (16).**

## DAILY SOLAR IRRADIANCE DATA FROM RWANDA

Yearly insolation is useful for estimating the amount of power available for a customer to use but when rating component sizes for the design of a solar home system the instantaneous power is more important. Figure 16 shows measurements taken from an e.quinox Energy Kiosk in Minazi, Northern Rwanda. Whilst the data does not show instantaneous power the data has 10 min resolution which is better than annual data.

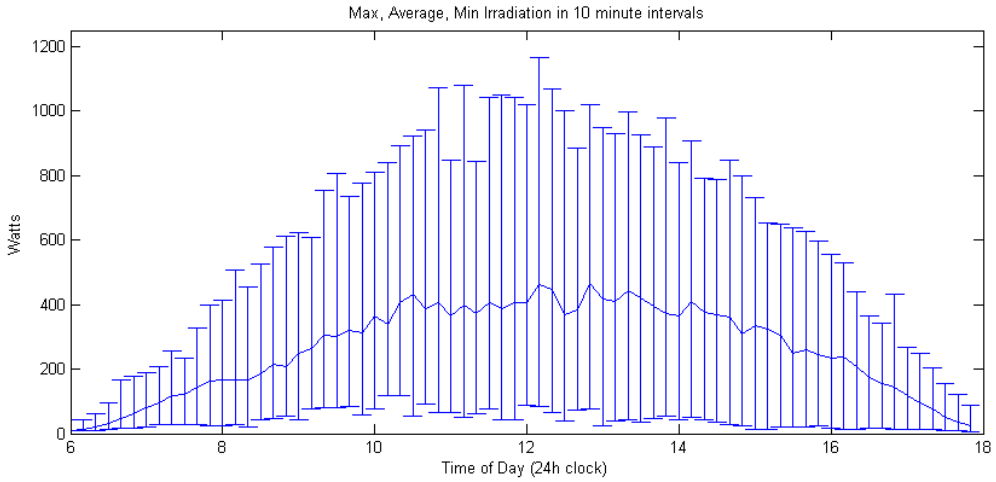


**FIGURE 16- SOLAR IRRADIANCE MEASUREMENTS FROM MINAZI, NORTHERN RWANDA. THE GRAPH SHOWS MAX, MEAN AND MINIMUM VALUES OVER 1 YEAR OF MEASUREMENTS. (17)**

Figure 16 show peak irradiance of 1166 W, giving a maximum achievable power from a 7 $W_P$ panel of 8.16 W. It is important that the system design is rated to at minimum this power rating but ideally greater to account for measurement inaccuracies, rating tolerances and higher than expected irradiance values.

## Sealed Lead Acid Batteries

Many battery technologies were explored for use in this product, the three best options are Sealed Lead-acid (SLA), Nickel-Metal Hydride (NiMH) and Lithium-Ion (Li-ion). A short comparison of the technologies is shown in Table 1.

**Table 1 - Comparison of Battery Technologies (18).**

| | SLA | NiMH | Li-ion |
|---|---|---|---|
| **Gravimetric Energy Density (Wh/kg)** | 30-50 | 60-120 | 110-150 |
| **Cycle Life** | 200-300 | 300-500 | 500-1000 |
| **Typical Cost for comparable capacity** | $25 | $60 | $100 |
| **Self-discharge / Month** | 5% | 30% | 10% |
| **Availability in Rwanda** | High | Low | Medium |

Sealed lead-acid batteries are the best option in terms of cost, availably and self-discharge but fall short in energy density and cycle life. The energy density is not of large concern as the izuba.box is expected to remain stationary in the customer's home. Cycle-life however is of more concern but the aim of this project is to increase this cycle life with intelligent charge management. Based on these considerations SLA batteries are the best choice for this application. However, if the cost of Li-ion continues to fall due to the uptake of use in electric vehicles then at some point in the future this may present the best option for off-grid solar systems.

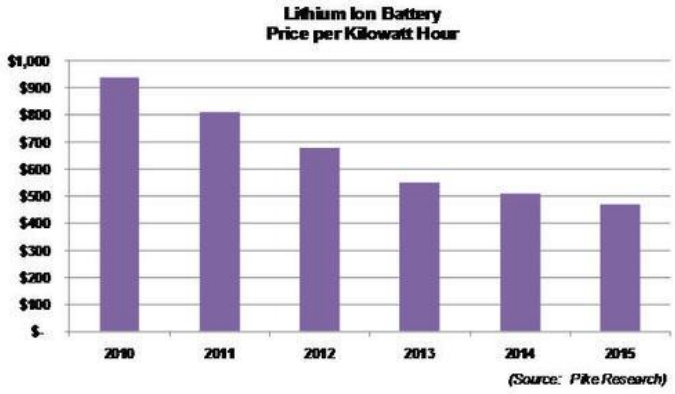


**Figure 17 - Trend of Li-ion Battery Prices (19).**

Lead-acid batteries work by submerging a pair of lead plates within sulphuric acid. There is a positive sponge lead plate and a negative lead dioxide plate with a separator between them, all submerged within the sulphuric acid electrolyte. Each pair of lead plates are called a cell and multiple cells are connected in series to make a battery. For a standard 12V battery 6x2.1V cells are used.

The discharge equation for a lead acid battery are:

$$Positive\ Plate: PbO_2 + 3H^+ + HSO_4^- + 2e^- \rightarrow PbSO_4 + 2H_{2O}$$

$$Negative\ Plate: Pb + HSO_4^- \rightarrow PbSO_4 + H^+ + 2e^-$$

On both plates the solid conductor reacts with the sulphuric acid to form the non-conducting lead sulphate on the plates. This is reversed during the charging reactions (20).

Batteries have two estimators of current state. The state of charge (SOC) shows the short-term, reversible state of the battery whereas the state of health (SOH) shows the longer term, irreversible state of the battery. Both are measured by comparing the current state of the battery with the state of the battery when it is fully charged (100% SOC) or when it was new (100% SOH).

## State Of Charge Estimation

State of Charge measures the short term state of the battery, the amount of charge remaining.

$$SOC = \frac{Remaining\ Capacity}{Capacity\ of\ Fully\ Charged\ Battery}$$

The most accurate method for measuring SOC is to measure the internal parameters of the battery, such as the ion concentration in electrolyte or the active mass parameters. There is a linear relation between ion concentration and SOC, however this requires the use of special, internal battery sensors which are expensive and not practical for this product.

SOC, in this product, must be estimated using external parameters such as voltage, current and temperature. Open-circuit voltage of the battery terminals has a simple relation to state of charge however the battery must be rested for five or more hours before an accurate measure of open-circuit voltage can be taken. This is not practical to use whilst charging or discharging a battery (20).

$$SOC = \frac{a - U_0}{a - b}$$

**Where $a$ is 100% SOC open circuit voltage, $b$ is 0% SOC open circuit voltage and $U_0$ is current open circuit voltage (20).**

A second method for SOC estimation is charge balance or Amp Hour counting. This allows for in-use estimation of SOC which is much more practical but less precise than using the rested open circuit voltage.

$$Q_b = \int_t I_{MR} \cdot dt$$

**Where $Q_b$ is the charge balance and $I_{MR}$ is the main reaction current (20).**

$$I_{MR} = I_{BATT} - I_{LOSS}$$

$$I_{LOSS} = i_{BAT} * (CF - 1) for\ charging$$

$$I_{LOSS} = 0\ for\ discharging$$

**Where $CF$ is the charge factor 1.0 < $CF$<1.2 (20).**

Using a Charge Balance technique to estimate SOC accurately is difficult as the integration of current needs to be done very accurately over a long period of time, otherwise small errors will accumulate and the SOC estimation will have a large error. Also, SOH needs to be accounted for in

the equations so occasional calibration is needed which involves a full charge cycle of the battery. Learning and calibration algorithms can be applied to the charge balance technique for estimating SOC.

## State of Health Estimation

State of health measures the current capacity of the battery against the capacity when new (or more exactly a few cycles after new as the battery settles in). The batteries capacity reduces over the lifetime due to many failure mechanisms which will discussed later in this report.

$$SOH = \frac{Measured\ Capacity}{Rated\ Capacity} (20)$$

Measuring SOH is difficult for similar reasons to measuring SOC. One method is using AHr counting whilst full discharging and charging a battery measuring the current capacity. An alternative method if to use the internal resistance as a SOH indicator. One paper suggests using a combination of AHr counting and internal resistance measurements to estimate SOH (21).

## Battery Lifetime Optimisation

Battery lifetime is affected by temperature of operation, usage characteristics, battery chemistry and internal design. These factors are out of the control of the system designer and can only be affected when choosing which batteries to purchase. Other factors within the system designers control which significantly affect battery lifetime is the level of discharge to which the battery is used and the characteristics of the battery charging.

Depth of Discharge (DOD) is one of the major considerations to make when optimising battery lifetime. The higher the DOD the shorter the lifetime of the battery. In one study of sealed lead-acid batteries a 20% DOD resulted in 4000 cycles before the battery was at the end of its serviceable life whereas a 100% DOD only lasted 27 cycles (22). There is a trade-off when choosing the DOD for a device, whilst a low DOD results in longer battery lifetime, the usable capacity of battery is reduced. This reduction in usable capacity can be countered by using a large battery however this must be balanced against cost, physical size and weight.

As a lead-acid battery is discharged lead sulphate ($PbSO_4$) is formed on both plates as shown in the discharge equations. This is a non-conductive substance. The further a battery is discharged the more lead sulphate is formed, in normal discharge the lead sulphate forms in a non-crystal state which easily converts back to lead and lead oxide when charged. If the battery is deeply discharged or left discharged for prolonged periods the lead sulphate forms in large crystalline structures which do not easily take part in the charging equations. The sulphate crystals reduce battery capacity in many ways, firstly it reduces the amount of active reactants available in the charging and discharging equations and also physically blocks the surface of the lead plate from being exposed to the sulphuric acid. The build-up of lead-sulphate crystals may be partially reverse by applying high energy pulses of current to the battery which help to break up these large crystals (20). This process is known as De-Sulphation.

The second factor affecting battery lifetime is the level of overcharging allowed by the charge control algorithm. Overcharging a flooded lead acid battery produces hydrogen and oxygen which escapes from the battery. These chemicals are easily replaced by adding distilled water to the battery. In a sealed battery water cannot be added so this effect must be minimised. Sealed batteries have additional chemicals added which allows for the oxygen and hydrogen to recombine

and stay within the battery. If overcharge current is small then the recombination reactions can remain in equilibrium and little net gas is generated (20).

An “Evaluation of the Impact of the Different Charging Algorithms on the Lead-Acid Batteries Lifetime” has been presented in a paper by H. Yatsui *et al* (21). The paper compares the algorithms used within four commercial charge controllers. It was found that the best charging algorithm used a medium speed of charging in the first stage of charging and pulse-charging in the floating stage. This also provided fast rates of charging. The PDI charging technique, shown as the red traces in Figure 18 and Figure 19 increased the SOH by up to 40% over other charging techniques (21).

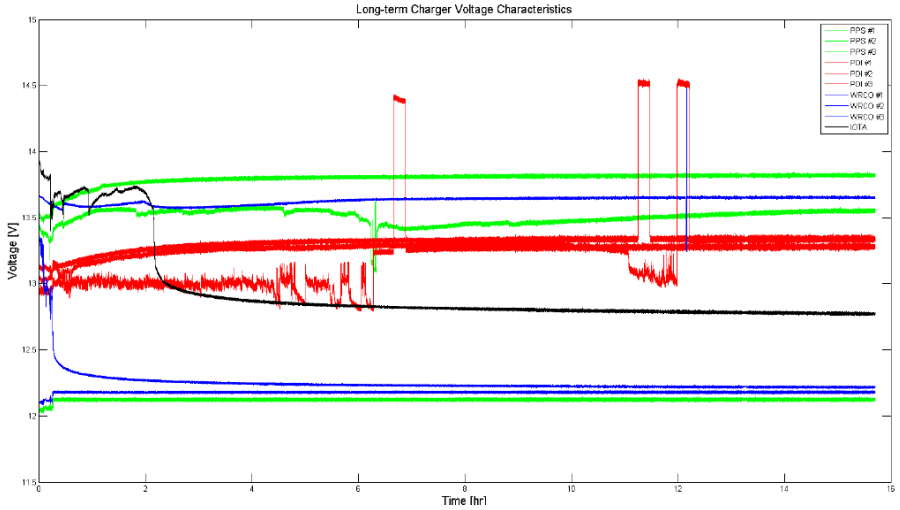


**FIGURE 18 – COMPARISON OF THE LONG TERM VOLTAGE CHARACTERISTICS OF VARIOUS COMMERCIAL CHARGE CONTROLLERS (21).**

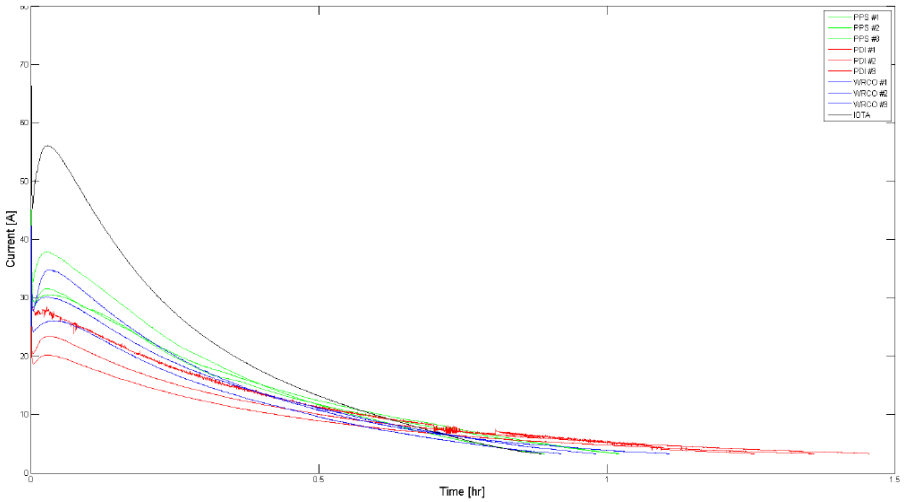


**FIGURE 19 - COMPARISON OF THE SHORT TERM CURRENT CHARACTERISTICS OF VARIOUS COMMERCIAL CHARGE CONTROLLERS (21).**

Figure 7 shows the current characteristics against operating voltage of a solar panel. Considering the operation of the most basic charge controller which simply connects the battery terminal to the solar panel terminals when the battery is not fully charged, we see that the charging cycle is

completely wrong for extension of battery lifetime. Rather than performing high current charging in the first stage and decreasing the charging speed as 100% SOC is reached, the most basic charge controller does the opposite. As the battery charges the terminal voltage rises bringing the operating point closer to the MPP, increasing charging current. This means that the current during overcharging is high leading to excess gas escaping from the battery. High currents during high SOC also make SOC more difficult to estimate as the voltage is further from the open circuit voltage.

## Lead-acid Charge Controller Topologies

Many charge controller topologies have been proposed in research papers and implemented in commercially available products. Armstrong *et al.* present a comparison of battery charging algorithms for photovoltaic systems (23). The three charging methods compared in this study are Intermittent Charging (IC), Three Stage Charging (TSC) and Interrupted Charge Control (ICC); their ability to maintain high state of charge, charging efficiencies and their temperature effects are compared. ICC is similar in concept to PDI charging which in the previous section was shown to increase SOH by up to 40% (21).

Intermittent charging is the most simple of the charge control algorithms, the battery is charged between two voltages thresholds, the battery is charged until the high threshold is met and then is left open circuit falls to the low threshold, at which point it is charged again. This can be performed with or without Maximum Power Point Tracking. The third party charge controllers purchased for use in the 2012 prototype izuba.box were of this type without maximum power point tracking (MPPT).

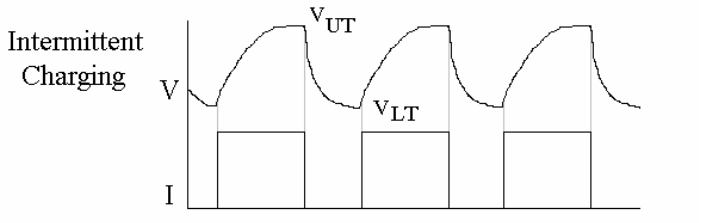


**Figure 20 - Voltage and Current Characteristics for Intermittent Charging with MPPT (23).**

Three stage charging splits the charging cycle into stages, the first charges the battery with maximum current until the battery reaches a set voltage called the absorption voltage. The second stage is slowly reducing the current whilst maintaining the voltage at the absorption voltage. The final stage is known as the float charging stage, this applies a small current to the battery and maintains the voltage.

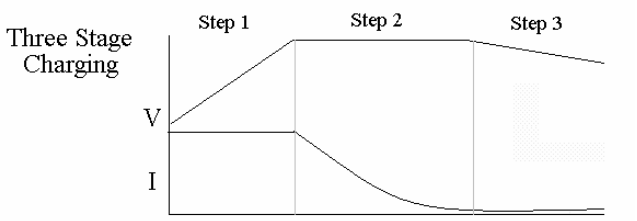


**Figure 21 - Voltage and Current Characteristics for Three Stage Charging with MPPT (23).**

Interrupted charge control is a variation on intermittent charging which has four modes, mode 1 charges at a constant current rate of $0.1C_{RATED}$[1] to an upper threshold voltage. It is then left open circuit until the battery settles at a lower threshold, at this point, mode 3 is entered in which the battery is pulse charged at $0.05C_{RATED}$ until the upper threshold is again reached. The fourth mode leaves the battery open circuit.

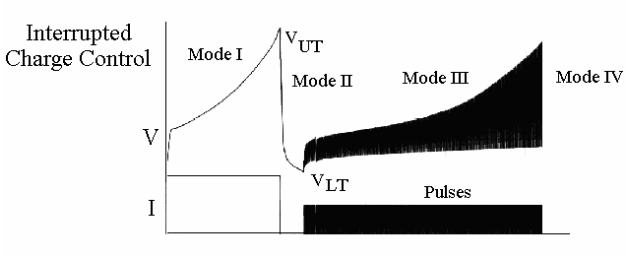


**FIGURE 22 - VOLTAGE AND CURRENT CHARACTERISTICS FOR INTERRUPTED CHARGE CONTROL (23).**

The results of Armstrong *et al's* tests showed that Three Stage Charging charged the batteries to 100% SOC quickest in no load conditions (Figure 23) and under load however in both cases over charged the batteries. We see that Interrupted Charge Control never over charges the batteries but also fails to charge the battery quickly due to the charging at a constant current rather than utilising the full power of the panel with MPPT.

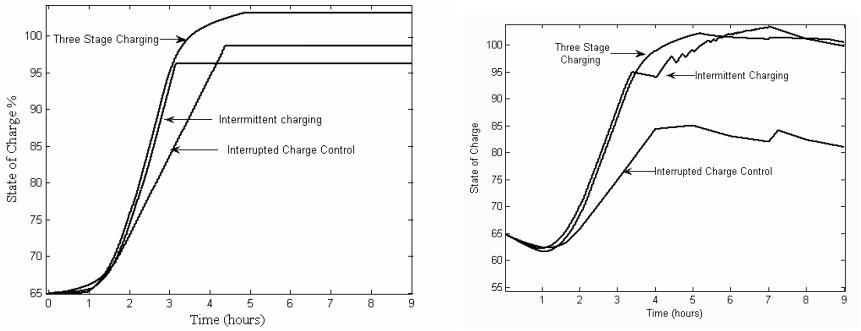


**FIGURE 23 – CHARGING TIME AND SOC COMPARISON FOR THREE CHARGE CONTROL METHODS (23). THE LEFT PLOT SHOWS A COMPARISON UNDER NO-LOAD CONDITIONS. THE RIGHT PLOT SHOWS A COMPARISON UNDER A VARYING LOAD.**

This project aims to implement ICC in a solar charge controller. The design must deal with the intermittencies of solar whilst using the ICC concept to prevent battery overcharging.

[1] $xC_{RATED}$ is the states Amp Hour (AHr) capacity of the battery by x. For example $0.1C_{RATED}$ Amps for a 7Ahr battery is 7*0.1 = 0.7A.

# Implementation

# System Overview

The izuba.box developed in this project can be easily separated into sub-systems as shown in Figure 24, whilst these sub-systems are partly independent they share many common resources such as a single microcontroller and power supplies. The most complex section of the system is the charge controller and this was the focus of the project. All electronics are brought together on a single PCB which also acts as the mounting for the user outputs and the LCD screen. The size of the PCB is limited by the size of the 7Ah battery used in the izuba.box.

Research into operation of the sealed lead-acid batteries and PV panels have been presented in the Background section of this report. This section will focus on explaining the implementation of each sub-section of the design. The charge controller takes reasonability for managing the battery and PV panel. It will include the DC-DC converter and charge controller algorithms.

The user interface section contains all parts of the system that the customer will interact will, this includes the LCD screen, keypad and power switch. The power switch does not cut power to the whole device, instead it is controlled by the microcontroller and will turn only the user interface and user outputs section of the device off. The charge controller and payment systems remain active but in low power states.

The payment system is tasked with managing the pay-as-you-go business model, it verifies any unlock codes entered and keeps a count of how much time has expired since the last payment. If payment expires a message is sent to the user outputs to turn off until a valid payment is entered.

The user outputs section provides two USB phone charging ports and three 12V DC outputs to the user for LED lighting. This hardware detects any faults on these outputs and disables them if necessary.

The full hardware designs can be found in the *Appendix Hardware Designs* section and is also hosted on Github at [github.com/equinoxorg/standalone_v2](github.com/equinoxorg/standalone_v2). Full software files are not included in this report to save space but can also be viewed at the above link if desired.

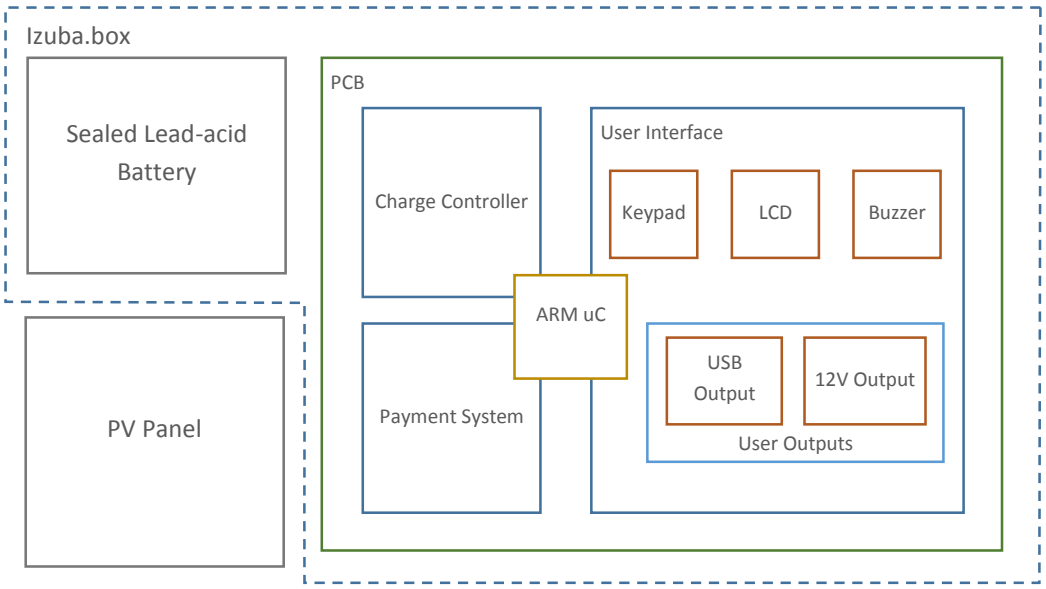


**Figure 24 - System Overview**

The final implementation of the izuba.box product has the following specification

- 12V 7Ah Sealed Lead-acid Battery
- 7$W_P$ Foldable PV Panel
- 3 x 12V 2.5mm DC Power Outputs (for LED Lighting)
- 2 x 5V USB DC Power Outputs
- 16x2 Character LCD Screen
- 3x4 Custom Numerical Tactile Keypad
- Tactile Soft Power Switch (with long-press reset)
- 2A Solar Charge Controller
- 2 x 2W LED Bulbs
- USB Multi-phone charging cable

FIGURE 25 - FULL IZUBA.BOX SYSTEM. DISPLAYED WITH 1 LED LIGHT AND USB CHARGER CABLE.

The power consumption of the designed system is shown in Table 2. This excludes the power consumption of any devices attached by the user.

TABLE 2 - POWER CONSUMPTION OF IZUBA.BOX SYSTEM

| State | Power Consumption |
|---|---|
| **On, backlight on** | 364 mW |
| **On, backlight off** | 230 mW |
| **Off, charging** | 218 mW |
| **Off, not charging** | 48 mW |

It is recommended that the system is fully charged and the battery disconnected from PCB when left unused for prolonged periods of time. A fully charged system will completely discharge if left connected for two months causing large sulphation of the battery and reduction in battery lifetime.

## System Cost

This product is designed to be sold in developing nations to price sensitive consumers, but the use of a pay-as-you-go payment plan makes this relatively expensive product affordable to many more customers. Typically the target for the payment plan is calculated so that the payback period is two-years and the customers pay less per week than they were previously paying for Kerosene.

The cost of the product is important as it should be able to return a profit whilst meeting the targets above. The costs of the system for a run of 100 units is shown in Table 3.

The largest single cost item is the assembled PCB followed by the faceplate. However the costs included in these two items include one-off design and tooling charges. Repeat orders of these components would bring the cost down.

**Table 3 - Breakdown of System Costs.**

| Item: | Notes: | Supplier: | Quantity: | Total Cost: |
|---|---|---|---|---|
| **Wooden Casing** | To be sourced on the ground | Rwanda | 1 | **£ 5.00** |
| **Casing Screws** | Wood Screws | Rwanda | 20 | **£ 1.00** |
| **Handle** | Plastic Handle with M8 Holes | RS | 1 | **£ 1.69** |
| **M8 Bolts** | To Secure handle | RS | 2 | **£ 0.60** |
| **7Ah Lead Acid Battery** | Shipped From China INCL Shipping | Bboxx | 1 | **£ 6.84** |
| **Key Pad** | E.quinox Logo Printed | China | 1 | **£ 0.98** |
| **PCB Stand/Nut/Bolt** | Hexagonal 14 mm M3 | Farnell | 4 | **£ 1.36** |
| **Battery Crimps** | One Red One Black | Farnell | 2 | **£ 0.12** |
| **Battery Wires** | One Red One Black | Farnell | 2 | **£ 0.10** |
| **Assembled PCB[2]** | Full component assembly | China | 1 | **£ 22.66** |
| **Foldable Solar Panel + Cable** | 7 Watt Panel From China | Bboxx | 1 | **£ 6.90** |
| **Metal Face Plate** | CNC Faceplate | Lincoln Binns | 1 | **£ 9.61** |
| **Box Labour Cost** | Wooden Box Construction Minazi | Minazi Community | 1 | **£ 4.00** |
| **Battery + Solar Panel Shipping Cost** | Shipping from China to Mombasa | Bboxx | 1 | **£ 1.91** |
| **Total** | | | | **£ 62.77** |

[2] A full breakdown on the electronics cost is shown in *Appendix PCB Bill Of Materials*.

# Microcontroller and Software Overview

The choice of microcontroller used in this product is one of the largest design decisions, the microcontroller must incorporate as much of the required functionality as possible whilst keeping cost and power consumption low. Many options were explored including Microchip's PIC series, NXP's LPC series and STMicroelectronic's STM32F0 series. The latter two are based on ARM's Cortex-M0 architecture.

It was decided that a Cortex M0 based microcontroller would be used for their high efficiency. The microcontroller used in the product was a STMicroelectronic's STM32F050C6, the reasons for this choice are many but the main advantage of this chip over other Cortex M0 chips was the price. As low as £1.00 in low volumes (24). This price is low in comparison to similar products from over vendors but unlike most alternatives includes real-time clock functionality. A discrete real-time clock costs between £2-3 in low volumes so the saving here is significant. A summary of the specification of the STM32F050C6 is shown in Table 4.

**Table 4 - STM32F050C6 Important Parameters (25).**

| Feature | Value |
|---|---|
| **Core Architecture** | ARM Cotrex-M0 |
| **Core Frequency** | 48 MHz |
| **Flash Memory** | 32 Kbytes |
| **SRAM** | 4 Kbytes |
| **Voltage** | 3.3 V |
| **Power Consumption [max]** | 396 mW |
| **Real-time Clock** | Yes |
| **Real-Time CLOCK Backup Battery** | Yes |
| **GPIO Pins (all mapped to interrupts)** | 39 |
| **ADC** | 12-bit |
| **ADC Channels** | 10 |
| **ADC Temperature Sensor Channel** | Yes |
| **USART Interface** | 2 |

One advantage of the STM32F050C6 is that there is a small range of devices with the same pin-outs and peripherals but with varying flash and SRAM capacities. This is useful as it is difficult to predict the amount of flash and SRAM required before completing the software development. In this project I approached the limit of the SRAM capacity so it could be sensible to switch to the STM32F051C8 which is a very similar chip but with 8Kbytes of SRAM and 64Kbytes of flash. These microcontrollers could be swapped with no alterations to the current PCB design.

## Software

The software development environment used for this project is ARM's MDK which includes ARM's C compiler and the Keil µVision 4 IDE. This is a paid for software but ARM has kindly provided a license to e.quinox for this project. However a free version is available with full functionality but a code limit of 32kB, the same size as the Flash memory of the STM32F050C6, thus this project can be developed and maintaining with free software (26). This is important as e.quinox and Engineers without Border aims to promote designs to other organisations to re-use and build upon under an open source model.

The decision to uses ARM's MDK rather than open-source alternatives was driven mainly by the RTX software included with the MDK. RTX is a real-time operating system (RTOS) which allows the

programmer to write code at a higher level. It allows the running of multiple *tasks* concurrently (based on time division multiplexing of system resources) which means the code is more simple to program and easier to maintain due to it being split into distinct and separate tasks.

The structure of the code can be broken down in a similar manner to hardware as shown in Figure 26. An advantage of using a RTOS is that each task can be tested separately, in this application it allows separate testing of the charge control algorithms, user interface and payment systems. It also makes the code more maintainable, for example if the product was altered to use Ni-Mh batteries rather than a sealed lead-acid only the charge controller task would need to be modified, all other tasks would remain the same.

Disadvantages of using a RTOS do exist and they include the reduced portability of code. Using ARM's RTX RTOS means that the code can be ported to other ARM devices but only as long as the MDK environment supports them. It would be very difficult to port the code to a platform with a non-ARM architecture as RTX would have to be replaced with an alternative RTOS.

A second disadvantage of using a RTOS is the overhead incurred in code space, memory requirements and computation time. When switching task the RTOS must store the state of the system, including all local variable onto the stack which takes time and memory space.

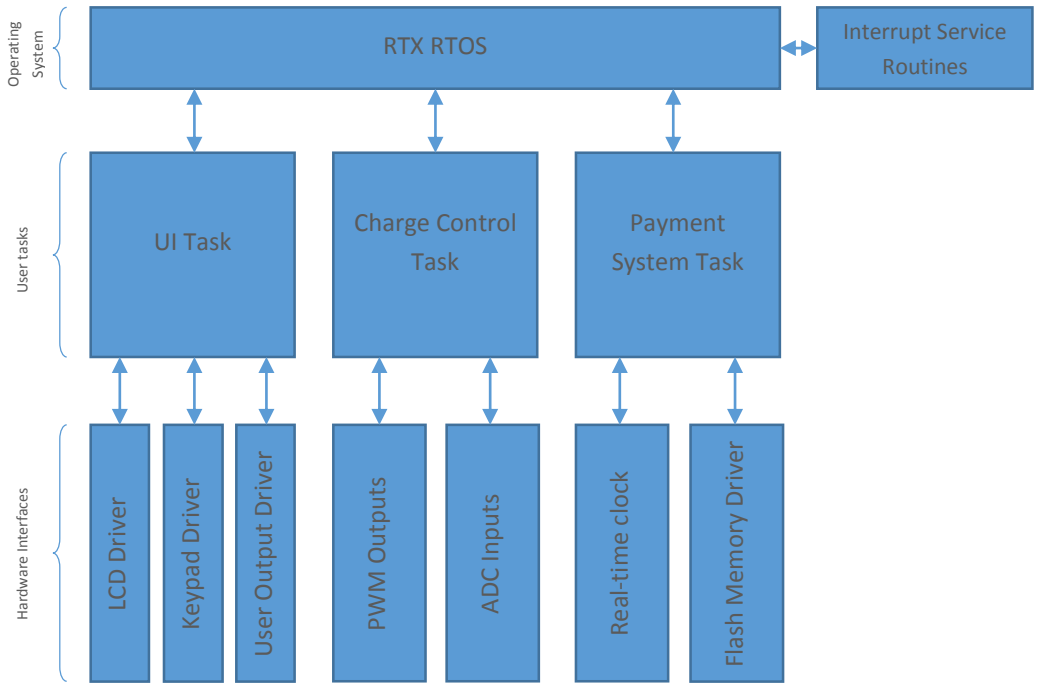


**FIGURE 26 – HIGH LEVEL STRUCTURE OF SYSTEM CODE**

Figure 26 shows the top level structure of the code and which task is responsible for controlling the shown peripherals. Some of the shared peripherals and less important details are missed for clarity. The following sections will discuss each task in more detail.

Communication between different blocks in the system occur in various manners, the simplest communication occurs between the tasks and the lower level drivers. The communication occurs through function call parameters. Communication between the RTOS, tasks and ISRs is more complicated. Tasks can have associated events, they can wait in an idle state until an event occurs

and then react accordingly. Events can be initiated by others tasks or ISRs but do not transfer any extra data with them. Mailboxes are another option for communication between tasks, other tasks can place data items in a mailbox and the receiving task can read and react to it. Mailboxes are used when more than a single event of communication is needed.

An example of an event is used in the keypad driver. An ISR is triggered when a key is pressed, this ISR sends an event to the UI task to tell it to scan the keypad, determine which key is pressed and deal with it appropriately. The benefit of using an event is that the ISR is very quick to complete and the action of a key can be determined by the UI task and can be dependent on other factors.

### Interrupt Setup

The STM32F0 series is based on the ARM Cortex M0 architecture which includes a Nested Vectored Interrupt Controller (NVIC) with 32 channels. These can be used for various peripherals such as the ADC and GPIO pins. Interrupts are used extensively for monitoring error conditions and user inputs to reduce the need for polling devices and for faster reactions to over current faults. Interrupts are also used to wake-up the device from low power states, this may be a timer event or a power switch event.

Interrupts are used for:

- SysTick for RTOS timing control
- Power Switch Event (This interrupt also wakes microcontroller from sleep or standby)
- Keypad events
- USB Overcurrent protection
- DC Output overcurrent protection
- Real-time clock alarm

## Code Safety

### Watchdog Timers

The code is written and tested in a defensive manner, meaning that any system lock-ups should be prevented by the use of timeouts. However, intermittent bugs may be missed and lead to lock-up of the microcontroller. To deal with lock-up failures Watchdog timers have been implemented. These are hardware decrementing timers which are reset to a high value periodically by the code. If a system lock-up occurs the timers will not be reset and after a set time will reach zero. If this occurs a hardware reset of the microcontroller will be performed. The chip can detect on start-up if the reset was due to a Watchdog timer and log the event to the serial port. This should help detect and fix bugs in future.

### Physical Reset Button

The Watchdog timer in the microcontroller should catch and deal with any system lock ups but will not prevent the system entering an unknown state or any other undesired behaviours. With careful coding and testing this should never happen but due to the nature of use of the product we want the user to be able to deal with any problems if possible. For this reason a physical Reset button has been multiplexed with the power switch on the faceplate. In the unusual scenario where the user needs to reset the device, the power switch must be held down for more than 5 seconds. This will cause a hardware reset of the microcontroller.

The chip has two pins of interest here, the first is a wakeup pin which is pulled high to soft power switch the device; the device will seem off to the user but the microcontroller will continue to run the charge controller code in the background. The second pin is a NRST pin, this will reset the microcontroller when pulled low.

Figure 27 shows the circuit diagram and simulation results of this power switch design. C1, R2 and M2 are used to time the 5 second interval, after C2 is charged for 5 seconds M2 will turn on. This will pull NRST low provided M3 is also on. M3 is on for all time that the switch is depressed, this means the reset line will be pulled high again as soon as the switch is released rather than waiting for C2 to discharge. V1 and M1 are simple used to simulate the power switch. R1 and C2 are the pull-down resistor and de-bouncing capacitor for the wakeup pin.

This design is extremely low cost as the switch is less than 20p in low volumes and the cost of the passives are negligible. The 2N7002 is also very low cost, less than 3p in low volumes.

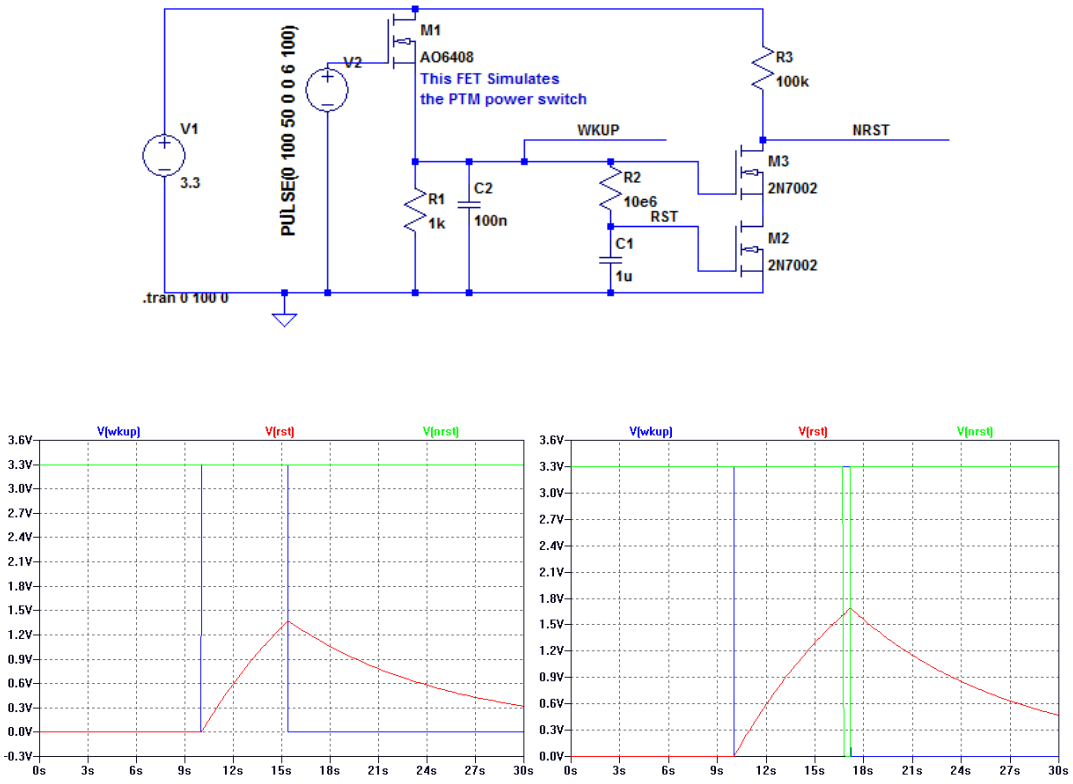


**Figure 27 - Two graphs showing the operation of the Power and Reset Switch. The Left Plot shows a Button Press of 4.5s and the Right shows a Button Press of 6s. In the 6s case the Reset line is pulled low.**

# Charge Controller

The charge controller is a combination of software algorithms and DC-DC converter hardware. The hardware used is a step-down (Buck) power convertor. This section describes the implemented hardware and software.

## Control Signals

The charge controller is controlled using the microcontroller which must take measurements from the solar panel, battery and temperature sensor as inputs and output a PWM control signal to the switch mode power supply circuit. These signals are filtered in both hardware and software to provide stable reading to the control algorithm.

### Voltage Sense

Voltage of both the battery and the solar panel must be read by the control algorithm. These should give an accurate reading of the voltage without noise. The main source of noise in the circuit is the 40 kHz switching noise from the MPPT hardware.

The voltage signals for both the Battery and Solar panel exceeds the 3.3V maximum input for the ADC. A simple potential divider has been used with RC filtering to overcome both of these issues.

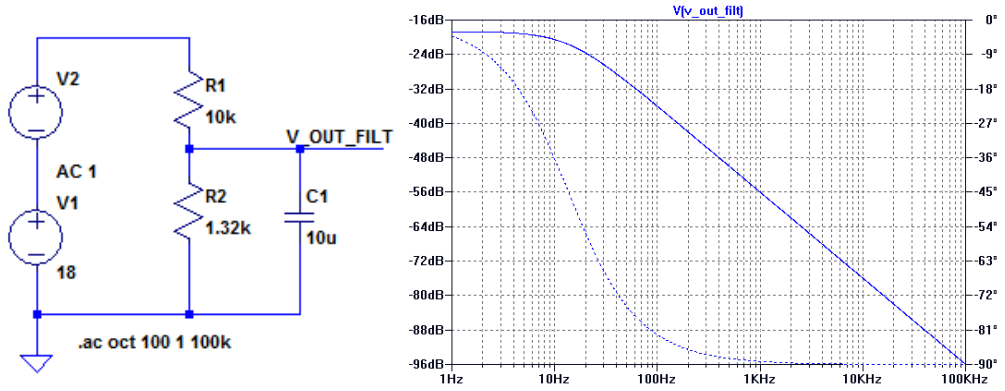


**Figure 28 – Voltage Sense Filtering Circuit and Simulation Results.**

### Current Sense

The current of the battery and solar panel must also be measured. The solar panel will only ever have a positive current so a unidirectional current sense amplifier is used in combination with a current sense resistor. Many current sense amplifiers are available but the ZXCT1107 was used for its attractive price point, small footprint, adjustable gain and minimal number of external passives needed. The gain of the ZXCT1107 is set using a single external resistor, $R_{GAIN}$ which is chosen to output 3.3V under the maximum expected current. The ZXCT1107 is a transconductance amplifier with transconductance $g_m$ = 0.004 (27). Filtering of the 40 kHz switching noise was added using C1 on the output.

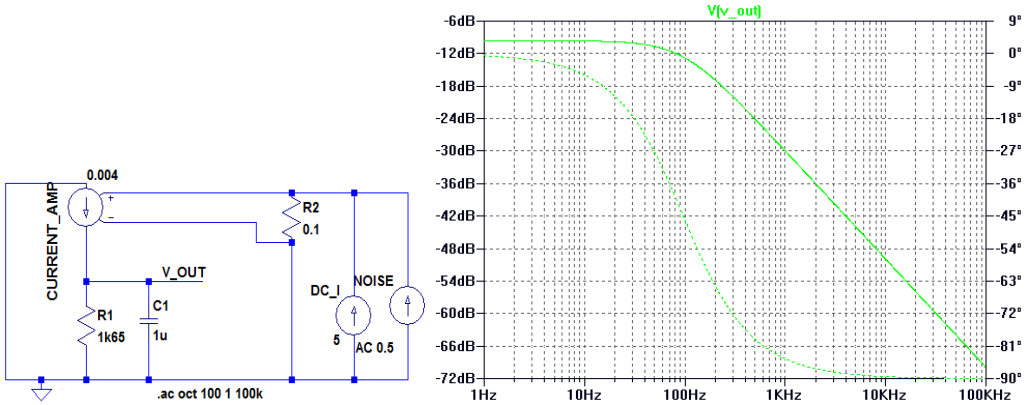


**FIGURE 29 - UNIDIRECTIONAL CURRENT SENSE AMPLIFIER WITH FILTERING. USED FOR PV PANEL CURRENT MEASUREMENTS.**

The current meansurments of the battery need to measure bi-directional current so that a single current sense can be used for both charging and discharging. The TI INA213 current sense amplifier was chosen for this aplication. Like the ZXCT1107 it has an attractive price point and small footprint but does require more external components. The INA213 has a voltage reference pin which is used to set the output voltage at 0A, in this application it is reasonable to set the reference as VCC/2 with a simple voltage divider. The voltage gain of the INA213 is a fixed 50, this means to change the current to output voltage scaling the sense resistor must be changed, in this application a sense resistor of 0.01Ω is used, giving a current to output voltage scaling of:

$$V_{out} = (I_{sense} * 0.01 * 50) + \frac{V_{CC}}{2}$$

Filtering of the 40 kHz switching noise is handled slightly differently with this current sense circuit. On the recommendation of the datasheet the filtering is placed at the input rather than the output. The advantages of this are that the low output impedance of the output buffer is not compromised (28). This filtering technique does result in a 0.84% gain error but this is not important as it is very small and the tolerances of the passives will be more significant. Errors can be calibrated in code if necessary.

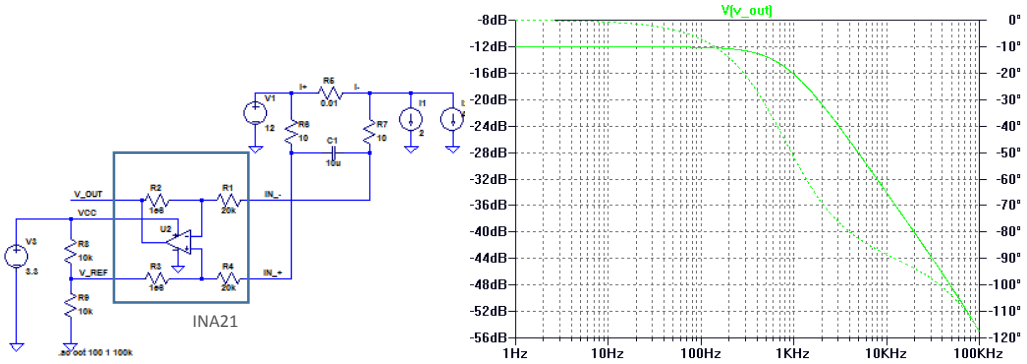


**FIGURE 30 – BIDIRECTIONAL CURRENT SENSE AMPLIFIER WITH FILTERING. USED FOR BATTERY CURRENT MEASUREMENTS.**

## ADC Setup

The ADC used is the microcontroller's internal ADC which is 12-bits and runs at 12MHz. The microcontroller is configured to measure 5 analogue voltages, these are:

- Battery Voltage
- Battery Current
- PV Panel Voltage
- PV Panel Current
- Internal Temperature Sensor

The ADC and temperature sensors are calibrated by STMicroelectronics's during production of the microcontroller and these calibration factors are loaded from read-only memory. Each ADC channel is sampled for 239.5 ADC clock cycles and the conversion takes 12.5 ADC clock cycles (29). This gives a maximum sampling rate of 47.5 kHz or 9.5 kHz for each channel.

To reduce the CPU overhead the ADC has been configured in continuous conversion mode meaning it will continually sample the 5 channels in a circular fashion. To further reduce the overhead, the ADC is coded to use Direct Memory Accesses (DMAs) to put the results of the ADC conversions directly into a circular buffer. When the charge controller task requires an ADC value the circular buffer is average then scaled to give a filtered voltage, current or temperature. The operation of the circular buffer is better shown in Figure 31. The benefits of this coding technique is that the ADCs run in the background with no CPU intervention until a value is required. At this point the average is calculated by the code does not have to wait to sample the ADC multiple times.

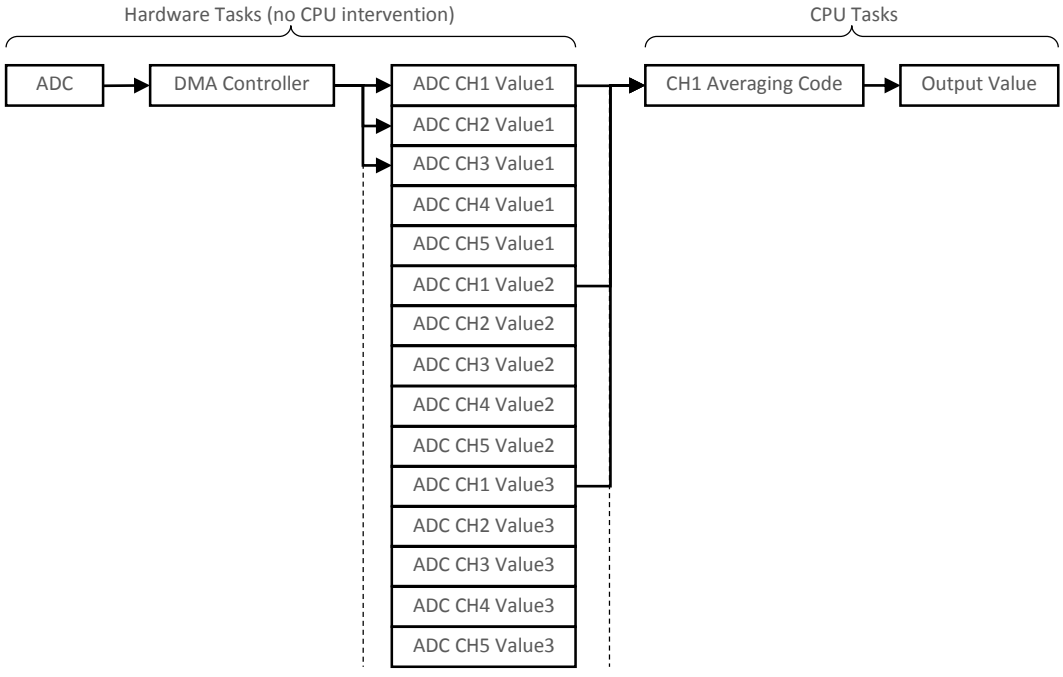


**Figure 31 - Operation of ADC in Continuous Sampling mode with DMA Access.**

The size of the circular buffer used is the number of channels * 16, which means that each ADC reading is the average of the past 16 samples, or the last 1.7ms. This combined with the hardware filtering makes the ADC readings stable and improves the operation of the charge controller.

## Buck SMPS

Figure 32 shows that the maximum power points for the izuba.box 7W PV panel under varying irradiance levels. It shows that the MPP is above 15V for useful power levels which is greater than the 14.4V maximum battery voltage. The DC-DC converter should only ever required a step-down in voltage so a Buck converter is used.

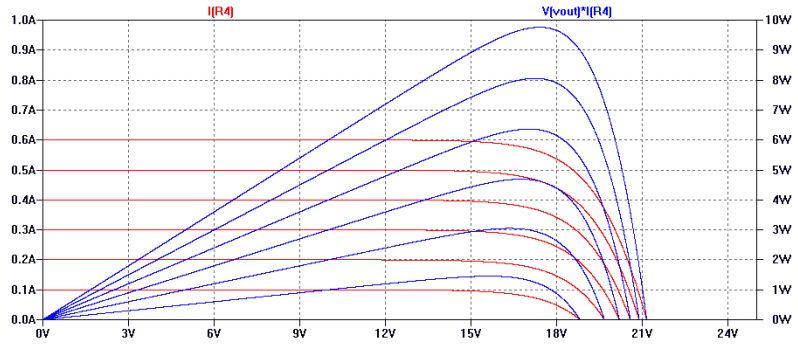


**Figure 32 - Power Curves of a 7W PV Panel Under Varying Irradiances.**

To make the charge controller design more versatile the hardware is designed to operate with a range of solar panel sizes, ranging from $7W_P$ to $25W_P$ but with an open circuit voltage, $V_{OC}$ of 21.8V. The short-circuit current for this range of panels is 0.45A to 1.8A. Looking back to Figure 16 we see that the maximum expected solar irradiance is expected to be 1166 W per $m^2$, which equates to an approximate maximum PV panel current of 2.1A.

The output current of the charge controller can be calculated with the maximum PV panel power and the minimum expected battery voltage. Any components on the output side of the buck convertor must be rated to at minimum, this current.

$$I_{out}^{max} = \frac{P_{peak} * \frac{Irrandience_{Max}}{1000}}{V_{Batt}^{min}} = \frac{25 * \frac{1166}{1000}}{10.5} = 2.8A$$

Voltage ratings of componenets are set by the open circuit voltage level of the PV panel and the battery which are 21.8V and 14.4 V maximum respectivly.

The values of the components used in the SMPS were calculated using TI's SMPS design tool (30) based on the known minimums and maximums for voltages and currents. The required values were found to be L=248µH and C=206µF. These values were then rounded to their next highest commonly available package, L=330µH and C=220µF.

These values were simulated using LTSpice including values for parasitics taken from datasheets. The model for a solar panel is described in the background research section of this report. The model for the battery is very simplistic but will act as a power sink at 11V.

Simulation results taken from this model are shown in Figure 34 and Figure 35. Figure 34 shows the results for the minimum expected input power from the panel based on irradiation data from Rwanda and PV panel parameters. Figure 35 shows results for the maximum expected input power.

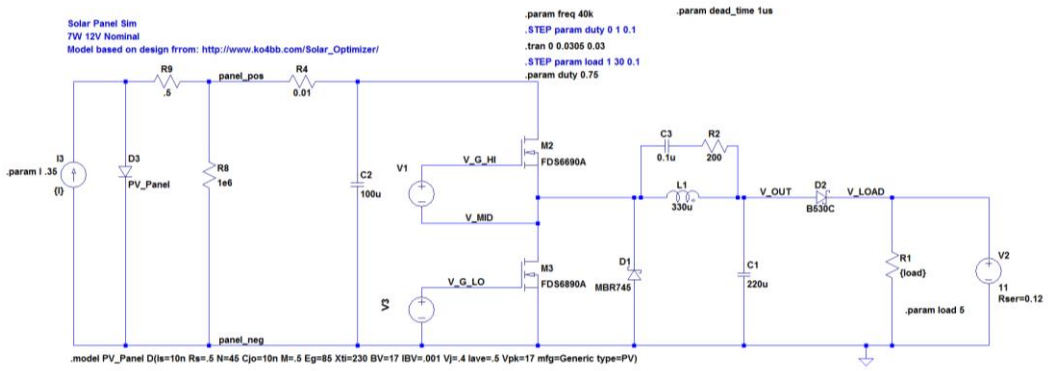


FIGURE 33 – LTSPICE MODEL OF CONVERTER HARDWARE.


FIGURE 34 - 0.05 I_SC PANEL. ROUGHLY EQUAL TO THE OUTPUT CURRENT OF A 7W PANEL AT 100 W/M^2 IRRADIANCE.

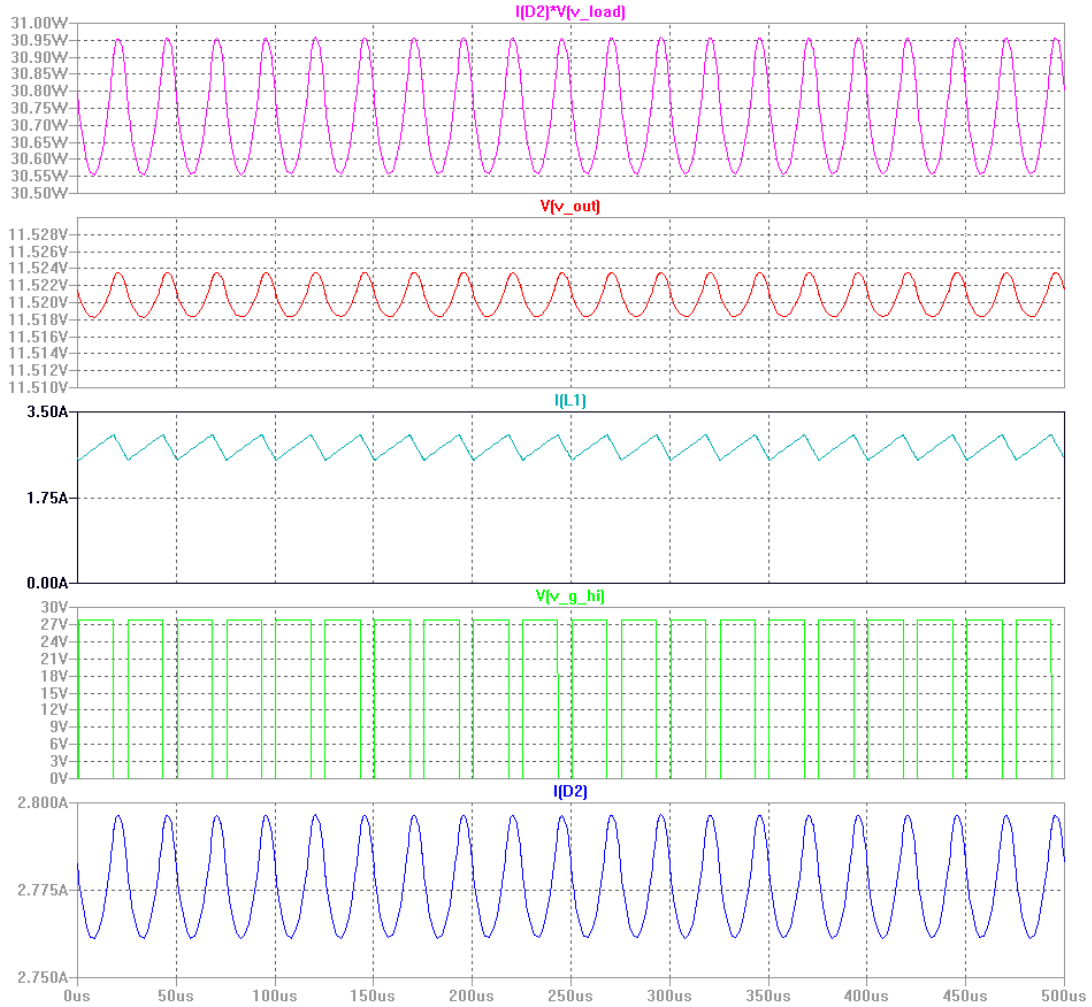


FIGURE 35 - 2.1A INPUT CURRENT. EQUIVALENT TO A 35W PANEL AT 1166 W /M^2 IRRADIANCE.

## EFFICIENCY

Using the simulation model shown in Figure 33 with the parasitic values taken from component datasheets, the expected efficiency of the converter can be calculated. The efficiency varies between 88% and 93% in the expected current range of the converter. A breakdown of which components consume the most power is more beneficial for improving efficiency. At peak power of 7W panel the efficiency break down is shown in Table 5.

TABLE 5 - SIMULATED EFFICIENCIES OF BUCK SMPS CIRCUIT

| DEVICE | POWER (LOSSES) | PERCENTAGE OF INPUT |
|---|---|---|
| **PV Panel Input** | 7.7W | - |
| **High Side Mosfet** | 11mW | 0.14% |
| **Low Side Mosfet** | 15uW | 0.0002% |
| **Inductor** | 250mW | 3.25% |
| **D1 (SMPS Diode)** | 20mW | 0.26% |
| **C** | 0.61mW | 0.008% |
| **D2 (Output Diode)** | 237mW | 3.1% |
| **Load** | **7.12W** | **92.5%** |

The two components which waste most power are the inductor and reverse current blocking diode. The inductor has a high series resistance of ~0.5Ω. It is possible to purchase an inductor with lower resistance however the cost and physical size of the device rises. The inductor used was deemed to give the best balance between cost and performance.

The diode used on the design is a Schottky type with 0.45 V forward voltage drop, the low forward voltage drop is used to minimise the power lost in this device. This reverse current blocking could be implemented with a Mosfet in active diode configuration in future which would reduce the power consumption but this must be balanced against cost.

## Interrupted Charge Control

Based on the research presented in this report, Interrupted Charge Control (ICC) was determined to be the most appropriate charge control algorithm for extension of battery lifetime. It was shown to overcome overcharging issues which is a major cause of reduction in usable lifetime of a sealed lead-acid battery.

ICC charges a battery in four modes, Mode 1 is a constant current (CC) mode at a current of $0.1*C_{rated}$ A and should charge the battery to over 85% SOC. Charging moves to Mode 2 when the battery exceeds an voltage threshold, Mode 2 is a battery rest state where the battery is left to fall to a lower voltage threshold. Mode 3 charges the battery with current pulses of $0.05*C_{rated}$ A. The pulses have 30s period and 33% duty cycle. Mode 3 will raise the SOC from 85% to 100%. Mode 4 is a fully charged state where the battery is no longer charged. When the battery voltage threshold reaches a restart voltage charging will be restarted in Mode 1. A plot of battery voltage and current during a single battery charge is shown in Figure 36 (31).

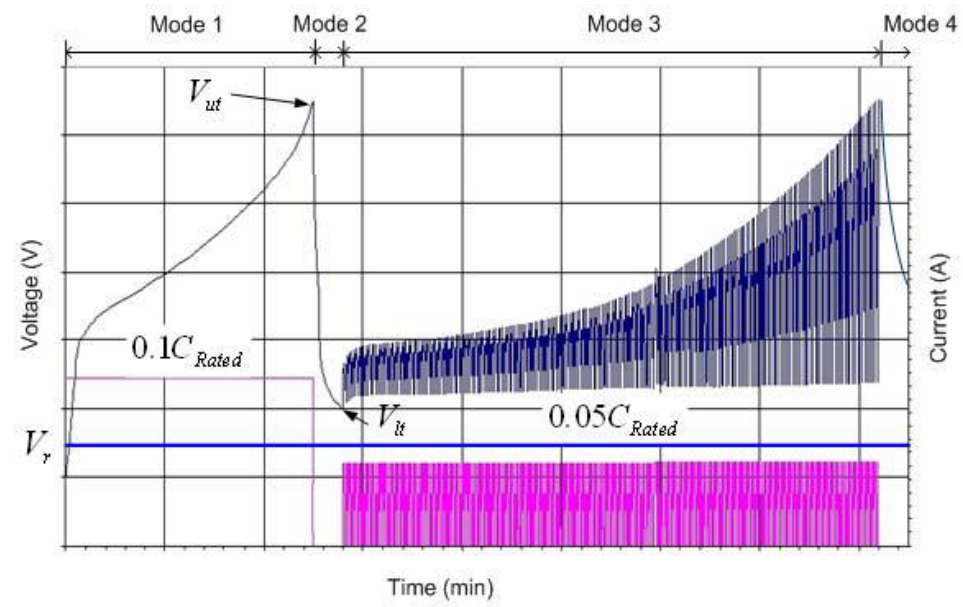


**Figure 36 – Operating Modes of the Interrupted Charge Control Algorithm (31).**

The ICC technique was originally designed with AC connected chargers in mind which means that the constant current conditions can be met. In a PV system the amount of available power is variable which means that at times the desired CC level cannot be met. In this situation standard MPPT will be used to keep the charging current as high as possible.

The algorithm used to set the duty cycle and thus the charging current of the battery is a modified perturb and observe maximum power point tracking algorithm. Under low irradiance conditions when the desired CC value cannot be met, the standard perturb and observe algorithm is used. Under normal irradiance conditions the algorithm increases the operating voltage of the solar panel until the target CC is met. This works as the PV power will fall if the operating voltage is pushed above the MPP thus the battery current will fall. The algorithm is shown in Figure 37.

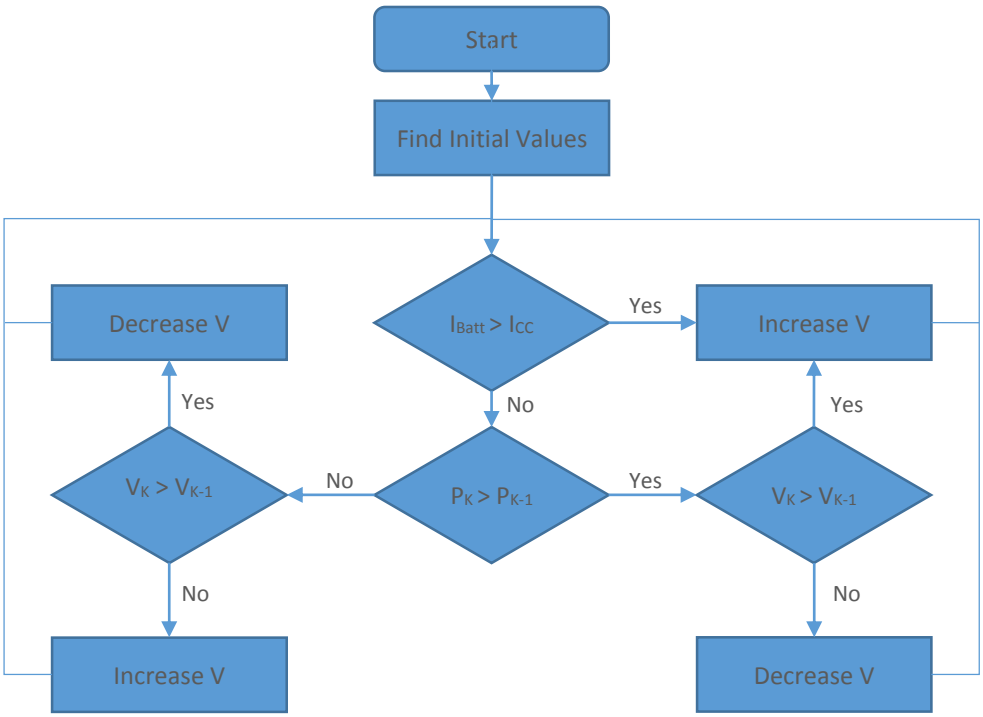


Where V is PV Panel Voltage, P is Power and k is the iteration.

**FIGURE 37 – FLOW CHART SHOWING THE PERTURB AND OBSERVE ALGORITHM MODIFIED TO CURRENT LIMIT WHEN EXCESS POWER IS AVAILABLE.**

The higher level algorithm which controls which mode the charge controller operates in is shown in Figure 38. The implemented algorithm adds a fifth state to Wong and Hurley's proposed algorithm to make it suitable for PV applications, the fifth state will be entered when the PV panel is producing negligible power, normally at night. This state allows the microprocessor and other hardware to enter a low power state and periodically wake to scan the panel for non-negligible power output.

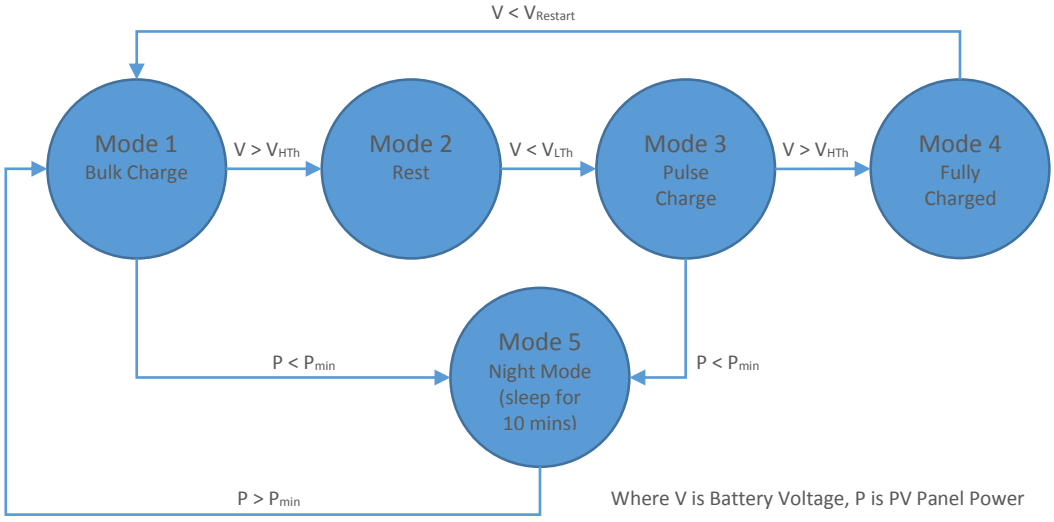


**FIGURE 38 – STATE MACHINE DIAGRAM SHOWING THE INTERRUPTED CHARGE CONTROL ALGORITHM.**

An important design choice for this algorithm is the choice of the threshold levels. The levels used are shown in Table 6 and were derived from research published on interrupted charge control (31). The threshold values are valid for a battery at 25°C and with the fully charging current available. They will be compensated to account for temperature and irradiance variations.

**TABLE 6 – THRESHOLD VOLTAGE USED FOR INTERRUPTED CHARGE CONTROL ALGORITHM (31).**

| THRESHOLD | BATTERY VOLTAGE |
|---|---|
| $V_{HTH}$ | 14.7 V |
| $V_{LTH}$ | 13.4 V |
| $V_{RESTART}$ | 12.8 V |

## TEMPERATURE COMPENSATION

Battery operation can vary with temperature and overcharging occurs at a lower voltage at increased temperature. Battery manufacturers give temperature compensation advice for three stage charging (Figure 39) but ICC needs a different technique method of implanting this.

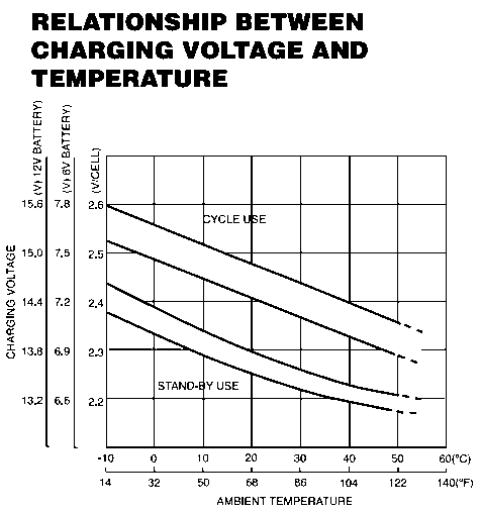


**FIGURE 39 - EFFECT OF TEMPERATURE ON BATTERY CHARGING VOLTAGES FOR THREE STAGE CHARGING (32).**

Temperature compensation of the voltage thresholds can reduces the rate of water loss and grid corrosion caused by to overcharging when the temperature is high. A suggested temperature compensation technique also changes the duty cycle of the charging pulse during the pulse charge state of ICC to prevent thermal runaway (33).

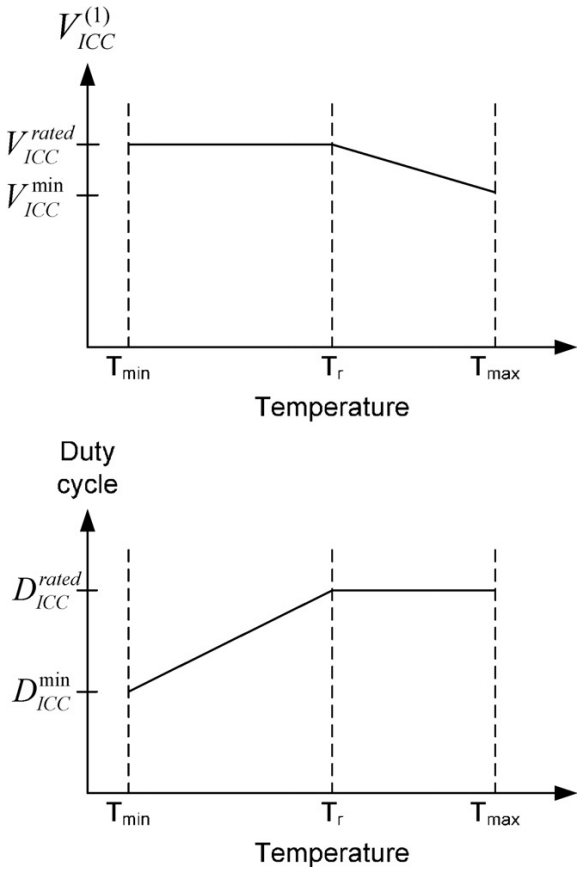


**FIGURE 40 - TEMPERATURE COMPENSATION FOR ICC (33).**

For the implementation in this project the parameters are shown in Table 7. These were derived from recommended values from the battery datasheet and a paper on ICC (33).

TABLE 7 - IMPLEMENTED TEMPERATURE COMPENSATION PARAMETERS.

| Parameter | Value |
|---|---|
| $V_{ICC}^{rated}$ | 14.7 V |
| $V_{ICC}^{min}$ | 13.2 V |
| $D_{ICC}^{rated}$ | 33 % |
| $D_{ICC}^{min}$ | 16.7 % |
| $T_{min}$ | 5°C |
| $T_r$ | 25°C |
| $T_{max}$ | 50°C |

## CURRENT COMPENSATION

ICC relies on charging a battery at a constant current until the high voltage threshold is met. Using a PV panel as the power supply means that at times this constant current target cannot be met. The battery can still be fully charged but at a lower current for a longer time. Figure 41 shows the effect of charging current on the threshold values, the graph is for three stage charging but by looking at the voltage values at 92% SOC the voltage thresholds for ICC can be derived. This introduces the problem that the voltage thresholds must be reduced for lower current charging levels.

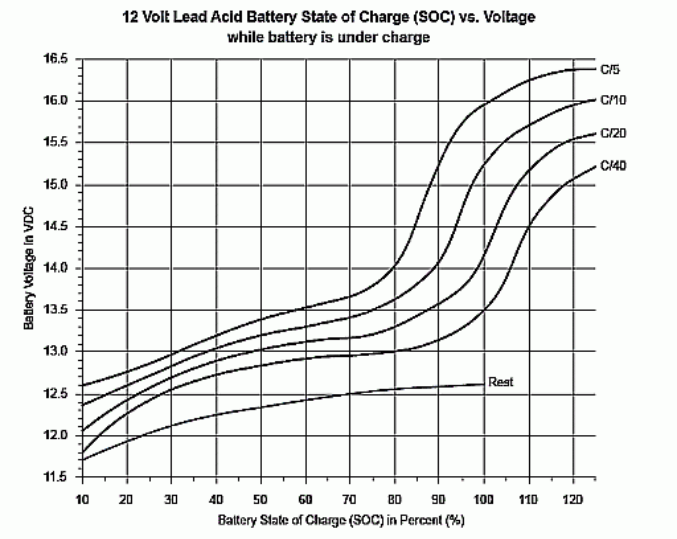


FIGURE 41 - EFFECT OF BATTERY CHARGING CURRENT ON VOLTAGE (34).

The voltage thresholds are compensated with the charging current as well as temperature as discussed above. The charging current is filtered to remove short-term drops in charging current due to cloud shading as battery voltage does not change instantly with changes in current. The values are compensated after the temperature compensation by multiplying the temperature compensated value by a scaling factor. The implemented scaling factor is shown in Figure 42.

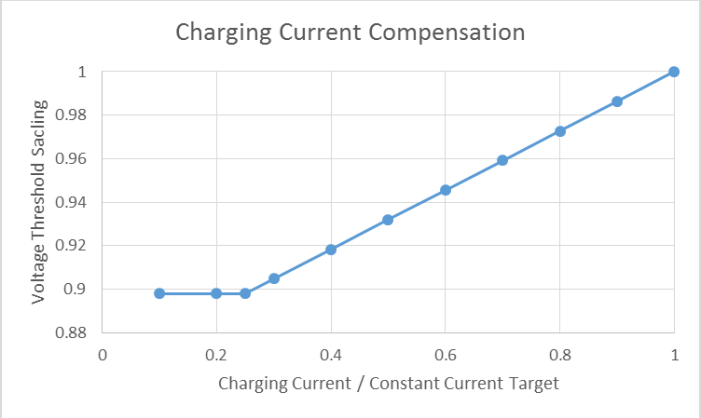


FIGURE 42 - CHARING CURRENT COMPENSATION OF UPPER VOLTAGE THRESHOLD.

## LOW VOLTAGE DISCONNECT

Research in the failure mechanisms of sealed lead-acid batteries highlighted two major causes of failure. The first is over charging and this has been addressed with the use of interrupted charge control. The second failure mechanism is over discharge of the battery leading to sulphation. Sulphation can be prevented by not allowing the battery to rest in a low SOC state, whilst the charging of the battery cannot be controlled, the depth of discharge (DOD) can.

When the SOC of the battery falls below a set level the outputs will be turned off and the user will be informed that the box cannot be used until recharged. The set point at which this happens is commonly called the Low Voltage Disconnect Level (LVDC) as is normally implemented as a single voltage threshold.

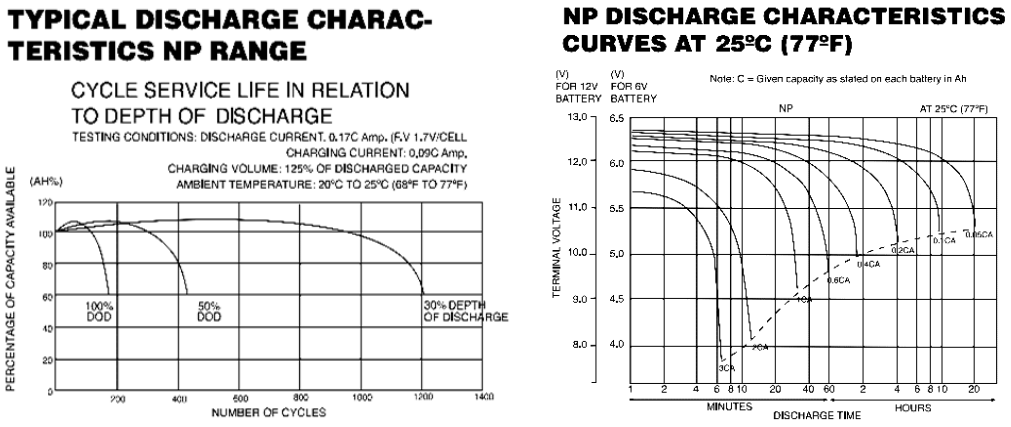


FIGURE 43 – DISCHARGE CHARACTERISTICS OF TYPICAL SEALED LEAD-ACID BATTERY (32).

Based on Figure 43 the disconnect voltage should change with output current. The graph showing the implemented disconnect voltages is shown in Figure 44. The voltage is constant below $0.1*C_{Rated}$ A and above $5*C_{Rated}$ Amps. It varies linearly between these two constants. The constant value at $5*C_{Rated}$ Amps is used to calculate the linear gradient but will never itself be required as the device limits output current to around $1C_{rated}$ A to prevent damage to the load switching Mosfets. The liner relationship makes the code implementation of the LVDC checking very simple and quick to execute.

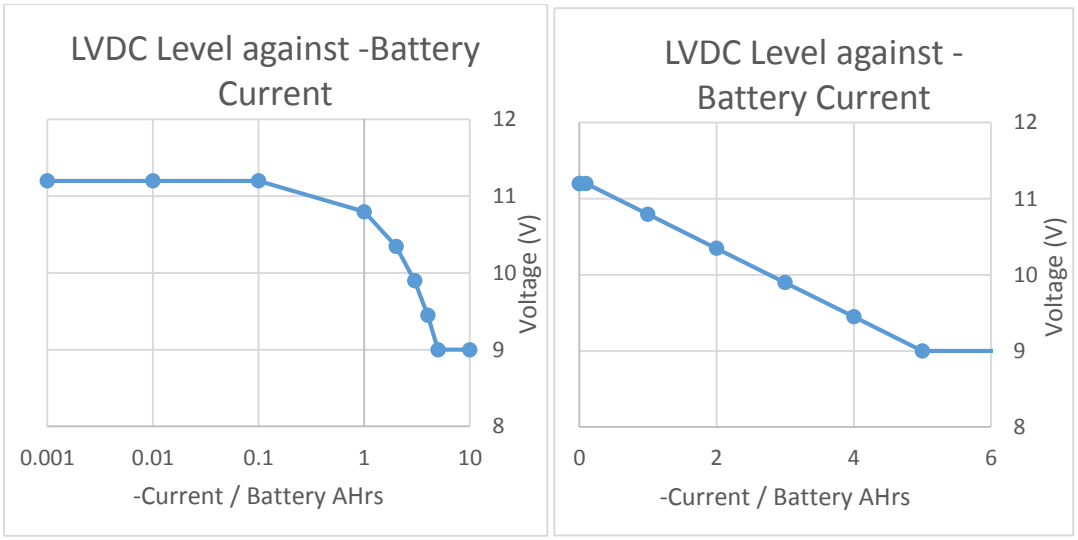


**Figure 44 - Cut Out Voltage Against Negative Battery Current. Negative Current is used as this represents Current out of the Battery, Positive Current is going into the Battery.**

The limits here are roughly set at 80% Depth of Discharge. However we do not expect this limit to be reached every day during normal use. Based on experience gained from the 2012 trial and e.quinox's experience with energy kiosks it is unlikely that a user will use more than 4 hours of 2W LED lighting per night, but may run two bulbs. They are unlikely to charge more than one phone per day. The total likely power consumption per night is 26 Wh. This roughly equate to a 30% Depth of Discharge on average which will help to prolong the lifetime of the battery. The LVDC level is a worst-case scenario and is designed to prevent the user from significantly shortening the lifetime of the battery.

## Results

The final implementation of the charge controller has been tested in many ways. Firstly the charging algorithm was tested by simulating a solar panel with a power supply. This allowed the charge controller to be tested with a predictable power supply that was not reliant on the weather.

A comparison has been made between a commonly used three stage charging algorithm and the implemented ICC scheme. Both charging batteries were matched in terms of manufacturer, age and starting state of charge. The comparison shows that both charge control scheme took 11 hours to full charge the batteries to 100% SOC with a rested open-circuit voltage of 13V.

Ambient temperature and battery temperatures were also recorded during the charging test to estimate the impact of the algorithms of battery lifetime without the need for long-term tests. The battery temperature corrected for ambient are shown in Figure 45. The results of this test are inconclusive as the precision of the temperature recording equipment was 1°C. The expected temperature difference between the charge control algorithms is expected to be less than 1°C.

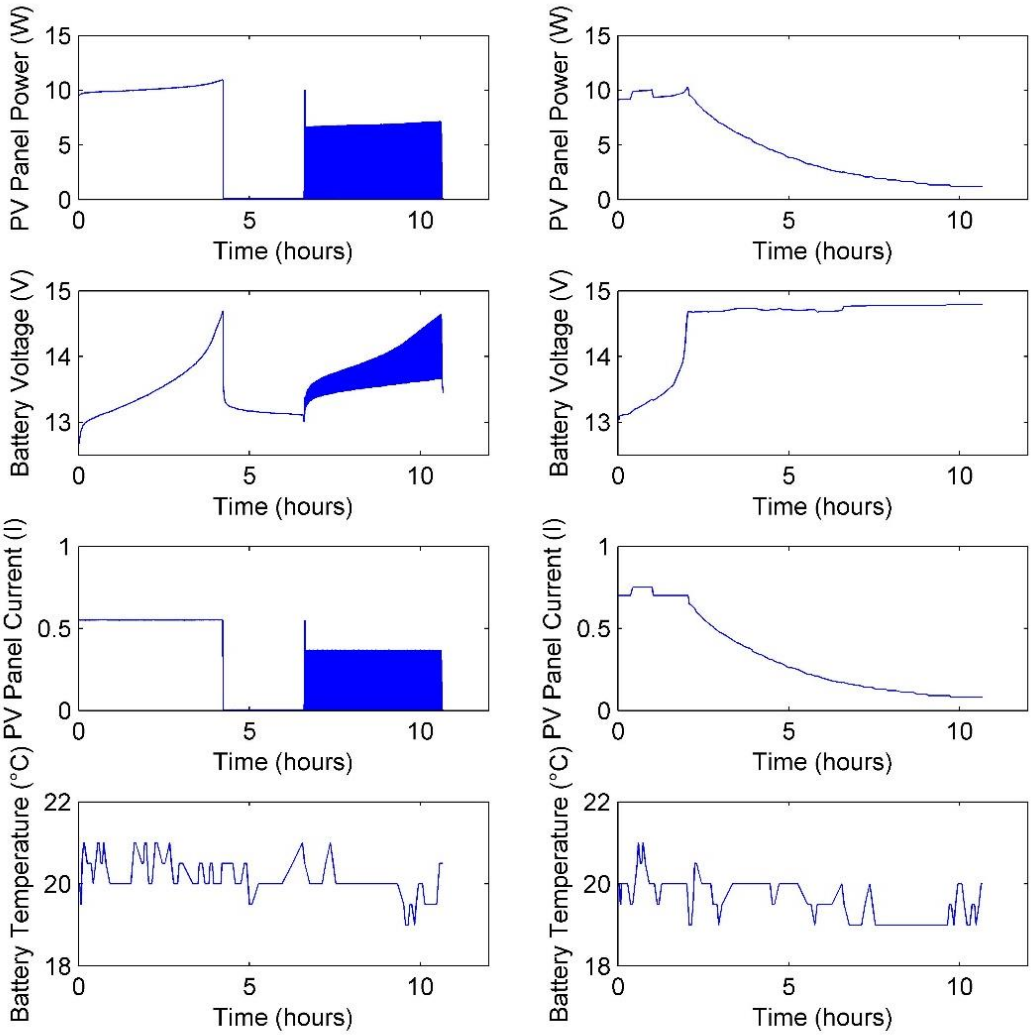


FIGURE 45 – COMPARISON OF THE IMPLEMENTED ICC CHARGING (LEFT) AND THREE STAGE CHARGING (RIGHT). COMPARISON WAS PERFORMED WITH SIMULATED PV PANELS WITH EQUAL POWER AVAILABILITY.

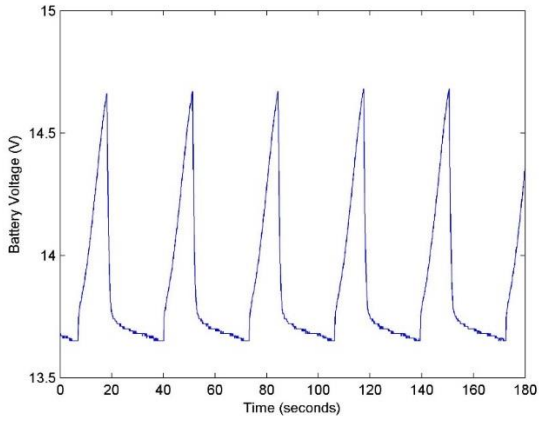


FIGURE 46 – ICC STATE 3, PULSE CHARGING. CLOSE-UP VIEW OF THE PULSE CHARGING STATE OF THE ICC ALGORITHM. 30S TIME PERIOD WITH 33% DUTY CYCLE.

The second testing technique was real-world testing over a two week period. The izuba.box prototype was used with a 7W PV panel mounted to a rooftop in Chelsea, London. This allowed the testing of the MPPT with non-constant lighting due to cloud shading and daily variations. Figure 47 shows the charging profile from a single day (31st May 2013). The plot shows the charge controller remaining is Mode 1 of the interrupted charge control algorithm due to the voltage never reaching the high threshold. At 17:45 irradiance falls away rapidly and the charge controller enters night mode. The drop in battery voltage is partly due to settling and partly due to a mobile phone being connected to charge.

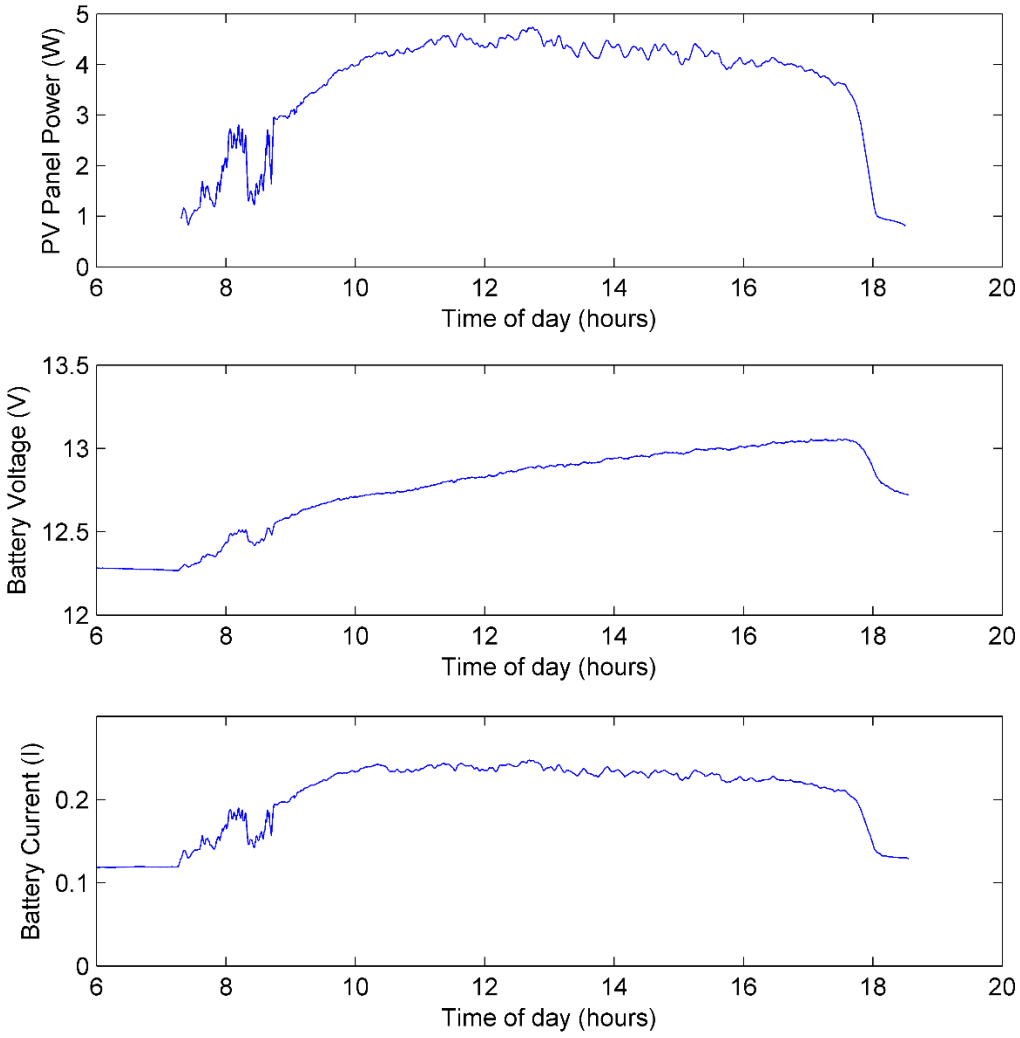


FIGURE 47 - PLOT OF PV PANEL POWER, BATTERY VOLTAGE AND BATTERY CURRENT FOR A DAY OF CHARGING.

# User Interface

The user interface is all aspects of the system that the user interacts with, this includes the LCD display, the keypad and USB and DC power outputs.

## LCD Screen

The main feedback to the user is though the LCD screen. It will display information such as the current SOC, Charging speed and time remaining until next payment.

The LCD screen is controlled by the UI software task which uses a LCD driver which was written specifically for this application and can display custom characters such as battery icons. The LCD has three states, the first state is the normal condition when the device is charged or charging and payment is valid. The second state is when a payment is required and the final state is a powered down state which is used when the box is off or in LVDC state.

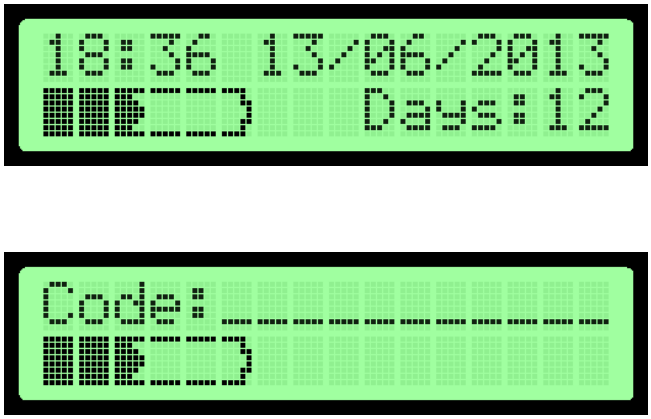


**Figure 48 - LCD States in Normal Mode (top) and Payment Required (bottom).**

The LCD shows the state of charge diagrammatically in a simple 5 steps of battery level. This is based on feedback from our first prototype in which people found a percentage figure confusing, especially if the battery level meter would vary by a few percent when a large load was plugged in. This solution is partly solved by more intelligent SOC estimation but also by simplifying the battery level display. A second advantage here is that the battery level indication is language independent. The battery icon is animated to indicate when the device is charging.

The LCD screen has two sources of power consumption, firstly the LCD uses power to display the characters on the screen, secondly the LCD has a backlight which consumers power when on. Measurements on a sample LCD gave the power consumption of the LCD to be ~5mW and the backlight to be 100mW. To reduce the power consumption of the izuba.box the LCD and backlight can be powered down separately by the microcontroller. The backlight is switched with a low cost Mosfets as shown in Figure 49. It is also possible to PWM the backlight to reduce the brightness and power consumption. The LCD is powered down with a command sent to the LCD. The microcontroller will power on the LCD when the box is turned on by the user, the screen will be off when the user turns the box off, even if the microcontroller is running the charge control algorithm. The LCD backlight is turned on with a 15 second time-out after a user event, such as powering on the box or interacting with the keypad.

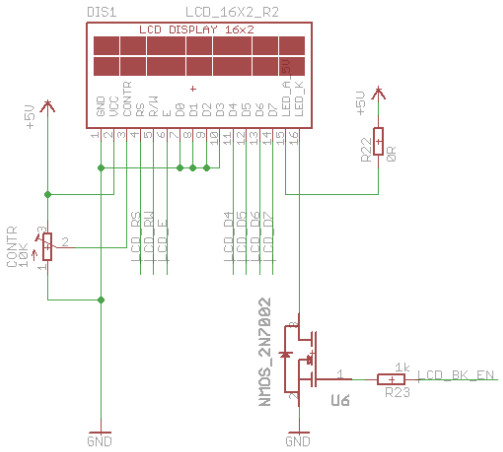


FIGURE 49 - LCD POWER CONTROL CIRCUITRY.

## KEYPAD

The keypad is custom manufacture by a Chinese supplier to the design shown in Figure 50. These have a self-adhesive backing and will be stuck to the faceplate. They keypads are connected to the PCB using a ribbon cable which passes through the faceplate underneath the self-adhesive backing.

As Figure 50 shows the electrical connection is a 3x4 matrix which connects to 7 pins of the microcontroller. The 4 horizontal connections are held low whilst the 3 vertical pins are weakly held high with pull-up resistors. When a button is pressed one of the 3 vertical pins is pulled low generating an interrupt in the microcontroller software. The interrupted causes the keypad to be scan be pulling only a single horizontal pin low at a time and detecting which vertical pin is pulled low. From this it can be determined which button is pressed.

The input from the keypad is predominately used for entering unlock codes into the device but can also be used to activate the LCD backlight for a short amount of time.

A small buzzer is included in the design which give the user audible feedback when using the keypad. It is also used as an alarm to indicate to the user that the battery is low or payment has expired.

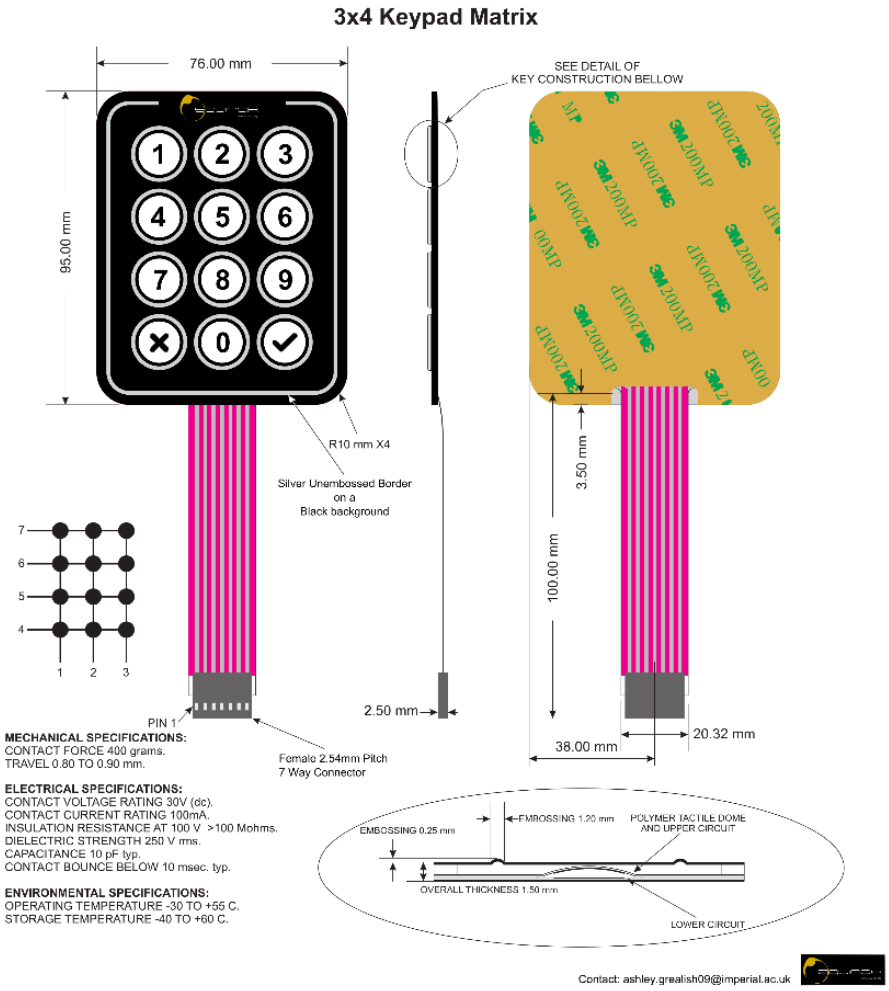


FIGURE 50 - KEYPAD DESIGN WITH EMBOSSED TACTILE BUTTONS AND SELF-ADHESIVE REAR.

## OUTPUTS AND PROTECTION

The outputs available for uses by the user are listing in Table 8. The DC sockets are designed to work with the 2W LED lights sold with the izuba.box but may also be used for other applications such as low power TVs. The USBs are designed for mobile phone charging but may be used to charge FM radios and any other USB powered devices.

TABLE 8 - POWER OUTPUTS AVAILABLE TO THE USER.

| Output | Quantity | Power Rating (each) |
|---|---|---|
| **12V 2.5mm DC Power Socket** | 3 | 1A |
| **5V USB Socket** | 2 | 0.5A |

FIGURE 51 – PROTOTYPE SYSTEM POWERING TV, LED LIGHT AND CHARGING A MOBILE PHONE

## USB OUTPUT PROTECTION

The USB sockets are powered by the 12V to 5V buck convertor which uses an LM2576 controller. This has a maximum output current of 3A and is used to power the USB sockets and is also used to power the LCD screen and the microcontroller through a 3.3V linear regulator.

The USB outputs are protected to allow a maximum current of 0.5A per output. If the connected device pulls more current than this or the USB socket is short circuited the output will be disabled by software. This current limiting is implemented using an AP1212 IC which is a high side power switch with overcurrent error flags. The error flags are linked to an interrupt service routine in the microcontroller which disables the USB output.

The USB data lines are voltage biased to indicate to connected devices that no more than 0.5A should be sourced from the USB port. This is simply implemented with a potential divider on each data line (35). This charger should be compatible with the latest smart phones (36) as well as the feature phones used in developing nations.

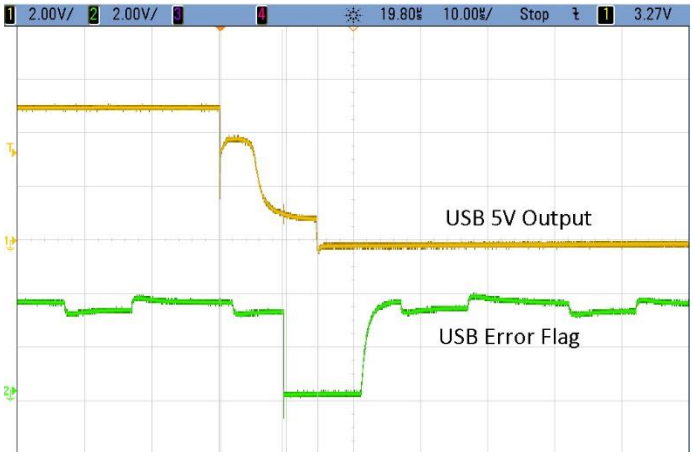


FIGURE 52 - USB OVER-CURRENT PROTECTION. MICROCONTROLLER REACTS TO ERROR FLAG IN 5µS BY DISABLING THE USB OUTPUT.

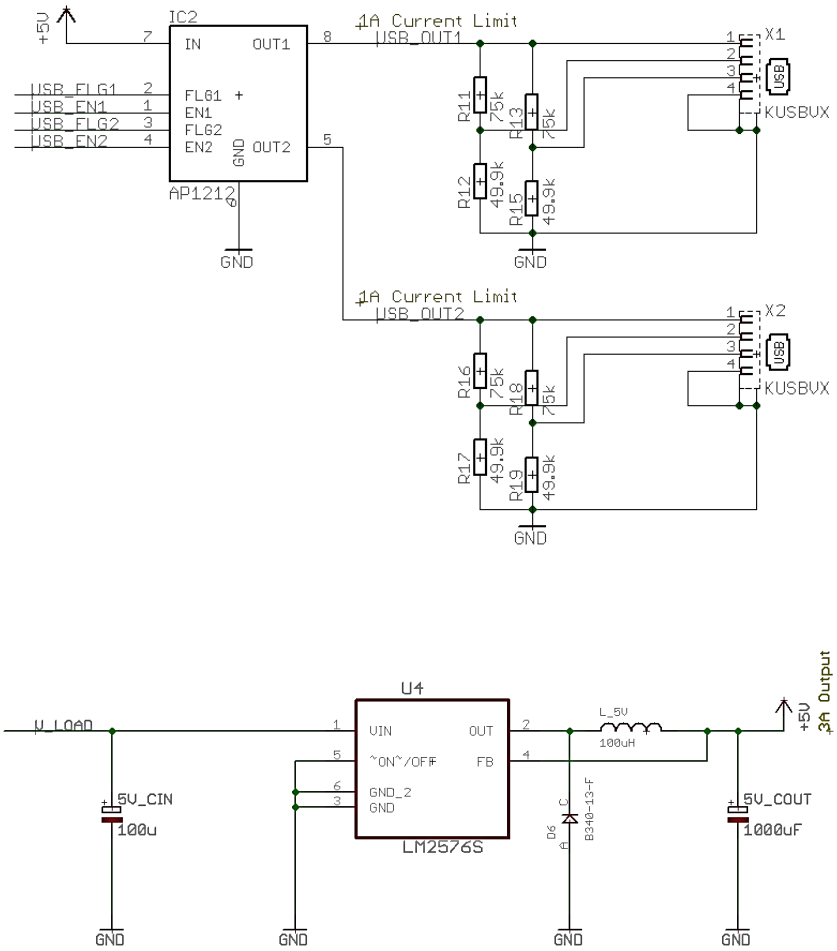


**FIGURE 53 - THE USB CHARGING HARDWARE. ERROR FLAGS OF THE AP1212 ARE CONNECTED TO INTERRUPT PINS OF THE MICROCONTROLLER.**

## 12V DC OUTPUT PROTECTION

The 12V outputs are not individually current limited but the current though all DC ports are monitored together and disabled if unsafe currents or short circuits are detected. The current is measured using the battery current sensing circuit.

The PV panel and Battery currents are read periodically by the ADC as described in the Charge Controller section. The UI task sets up an Analogue Watchdog on the Battery current ADC channel, if the measured current rises above a predefined safe value an interrupt will be generated. The interrupt will use the current battery current in combination with the PV panel current to decide if the output current is at an unsafe level. If it is the output will be disabled and the user will be informed. This will prevent failures which were seen in the 2012 izuba.box prototype which resulted from over-current on the DC output sockets.

## BATTERY SHORT CIRCUIT AND REVERSE POLARITY PROTECTION

Sealed Lead-acid batteries can ignite or explode when short-circuited for prolonged periods of time (37). The microcontroller code monitors battery current using the analogue watchdog described earlier but it important to add a hardware safety feature in case the short circuit causes the microcontroller power rail to be pulled down. This is could easily happen if moisture or any connective material shorts out metal contacts on the PCB.

A resettable fuse has been placed on the battery input line. This is designed to hold at up to 7A and trip at 16A so should not affect normal operation which limits above 5A. This is not designed to protect any circuit elements but to prevent dangerous battery short circuits if all other over-current protection has failed.

The battery is housed within the closed casing of the product and should never be changed by the user, however the boxes will be assembled by a local workforce so there is a small chance of battery terminals being incorrectly attached. To reduce this chance as much as possible the connector used for the battery can only be inserted the correct way into the PCB. The other end will be colour coded to match the battery terminals. Whilst this should reduce risk there may still occur human error in both the cable assembly and the final product assembly. A reverse polarity protection diode has been added to the battery input circuitry. This, along with the PTC should prevent damage from reverse battery connections at most there will be -0.7V from $V_{Batt}$ to Gnd which is within the safe levels for all components.

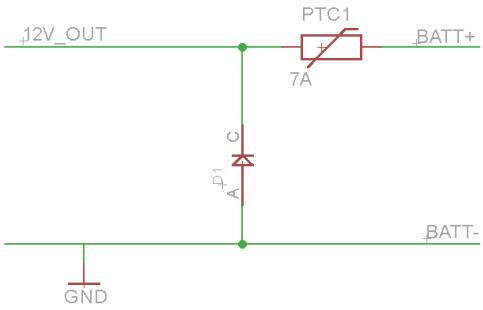


**FIGURE 54 - BATTERY HARDWARE SHORT-CIRCUIT AND REVERSE POLARITY PROTECTION.**

## PAYMENT SYSTEM

The customers of this product pay for the use of the outputs though a pay-as-you-go business model. They can purchase between 2 days and 2 months access at a time. The izuba.box must keep track of how much use the customer has paid for and also how much time has elapsed since the payment.

The customer pays for the product using a mobile money transfer system and e.quinox is currently in the process of producing an "app" for all feature phones based on the USSD protocol to simplify this process. Following payment the customer receives an SMS containing an unlock code which is typed into the product keypad. Once this is verified the box will unlock the outputs for the length of time paid for.

To ensure unlock codes are unique to each product and are only one time usable the software must store a box id and the number of times an unlock code has been used. These are also stored by the server which generates the codes and is transferred and verified as part of the unlock code. The Box ID itself is not transferred in the code but is used to generate the checksum, in this way if the code is used on a box with the incorrect box id then verification of the checksum will fail. The checksum is also generated from a shared secret field which is programmed on the server and in the microcontroller firmware but not transferred as part of the unlock code.

| Checksum | | | | | | | | | | | | | | | | Data Packet | | | | | | | | | | | | | | | |
|---|---|---|---|---|---|---|---|---|---|---|---|---|---|---|---|---|---|---|---|---|---|---|---|---|---|---|---|---|---|---|---|
| 31 | 30 | 29 | 28 | 27 | 26 | 25 | 24 | 23 | 22 | 21 | 20 | 19 | 18 | 17 | 16 | 15 | 14 | 13 | 12 | 11 | 10 | 9 | 8 | 7 | 6 | 5 | 4 | 3 | 2 | 1 | 0 |
| Checksum | | | | | | | | | | | | | | | | rand | | | | | Unlock_count | | | | | | | | Unlock_days | | |

**FIGURE 55 – BINARY STRUCTURE OF THE UNLOCK CODE. THIS IS SENT TO THE CUSTOMER AS A 10 DIGIT DECIMAL NUMBER**

The unlock days field tells the box how long the customer has paid for. It is a coded value between two days and 8 weeks. The full unlock code will be generated and issued when the customer has paid the full cost of the system. At this point the payment system will be disabled and the customer can use their box without purchasing unlock codes.

| Unlock_days | | | | |
|---|---|---|---|---|
| | 0 | 0 | 0 | Full Unlock |
| | 0 | 0 | 1 | 2 Days |
| | 0 | 1 | 0 | 5 Days |
| | 0 | 1 | 1 | 7 Days |
| | 1 | 0 | 0 | 2 Weeks |
| | 1 | 0 | 1 | 3 Weeks |
| | 1 | 1 | 0 | 4 Weeks |
| | 1 | 1 | 1 | 8 Weeks |

**FIGURE 56 - THE CODED VALUES FOR THE UNLOCK DAYS FIELD IN THE UNLOCK CODES**

The unlock code structure is the same as the structure used in the 2012 prototypes[3] however due to a change in hardware the low level drivers needed to implement these algorithms need to be re-written. The two largest changes are switching from an off-chip real-time clock to one incorporated into the STM32F0 microcontroller. A second change is from using internal EEPROM to internal Flash for non-volatile data storage.

[3] A separate e.quinox project is currently working to improve the security of the unlock codes.

## Real Time Clock

A real time clock (RTC) is used in this design to monitor the elapsed time since payment. The STM32F0 series microcontrollers incorporate a RTC as a peripheral. The clock source for the RTC is coded to be an external 32.768 kHz crystal with two 12.5 pF load capacitors shown in Figure 57. The 32.768 kHz is pre-scaled down to 1Hz by the microcontroller and drives the RTC.

A second battery (in addition to the main storage battery) is used to back-up the RTC in case of power failure or during times when the microcontroller is in sleep or standby mode. The RTC will continue to increment and the time will not be lost. This backup battery is soldered directly to the PCB to prevent any accidental or deliberate tampering which may occur by the customer. The back-up battery is expected to last 10 years, far exceeded the expected payback time for the product during which the RTC is required.

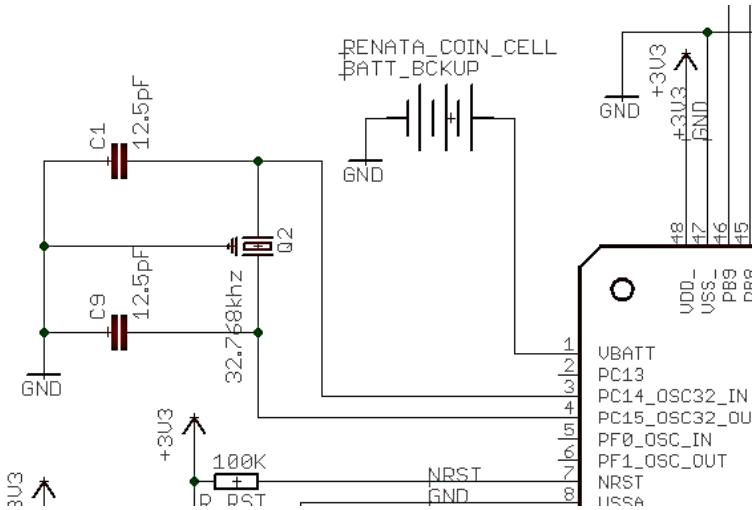


**Figure 57 - Schematic Segment Showing RTC Crystal and Back-up Battery connected to the STM32F0 Microcontroller.**

## Non-Volatile Memory

The product must store a range of variables such as the ID of the box and the number of times it has been unlocked. These values must be retained even when power is removed from the PCB. For this reason SRAM cannot be used, two options for storing these values are an External EEPROM IC or partitioning the Microcontrollers flash memory and using one partition for an Emulated EEPROM and the other for code space.

Flash Memory is on-chip and is much faster to read than off-chip EEPROM but may take longer to write to as a whole flash page must be erased and re-written for every write. As this non-volatile memory will only be written to when a new unlock code is entered the extra time required for a write is not significant (38).

A Flash memory write can be interrupted by a Microcontroller reset or a power supply failure. To prevent corruption of the stored variables two Flash pages are written to separately, if one becomes corrupted the other is used to restore it; this may lose the last data item to be written but will recover all other data.

## Design For Assembly

As discussed in the introduction to this report, the secondary aim of the project is to design the izuba.box to reduce manufacturing time and increase durability. The product should be suitable for other organisations to have produced by our partner suppliers without expert electronics or manufacturing knowledge. The only exception to this is the rear wooden case which we will have manufactured by potential customers in Rwanda under the guidance of a local carpenter. If this cannot be replicated by another organisation then the work to replace this with a factory produced metal casing would be minimal. E.quinox feels that local production of part of the casing is advantageous as it allows training of the locals in how to use and maintain these products and also serves as marketing.

### Casing

The casing of the unit was influenced by local tastes in the target deployment area, Rwanda. The rear of the casing is made from locally sourced wood and assembled by a local workforce. The layout of the casing was designed[4] to be as small as possible to reduce cost in both materials and transportation. The size of these units are limited by the size of the battery and all electronics are designed to be smaller than the largest face of the battery.

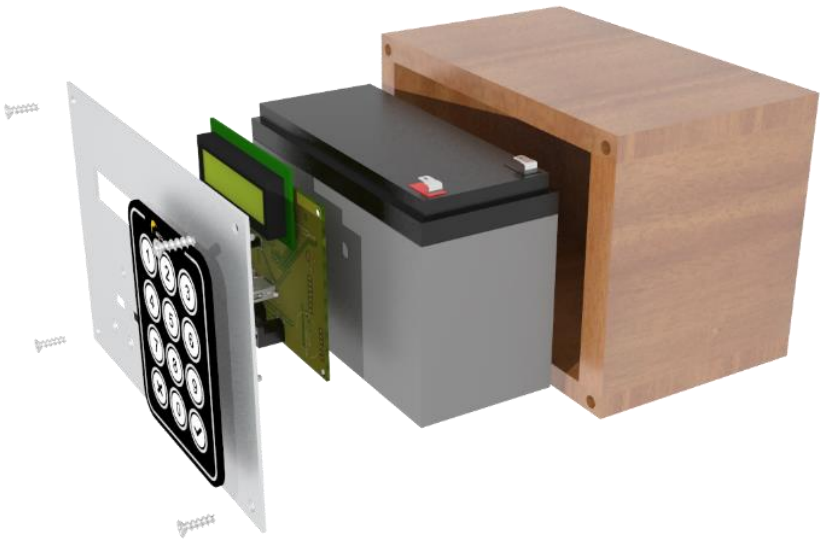

**Figure 58 - Exploded View of Full Izuba.Box Design**

### Faceplate

To prevent issues with poor tolerances and changeability of wood the faceplate is manufactured in the UK from Aluminium. Aluminium was chosen for its anti-rusting properties and wide and cheap availability. The faceplate with be sourced from a UK company, Lincoln Binns who will stamp sheet aluminium with the required holes.

[4] The layout of the faceplate was designed by myself but the CAD drawing and manufacture was kindly completed by Matthew Wood, Civil Engineer and e.quinox member, Imperial College.

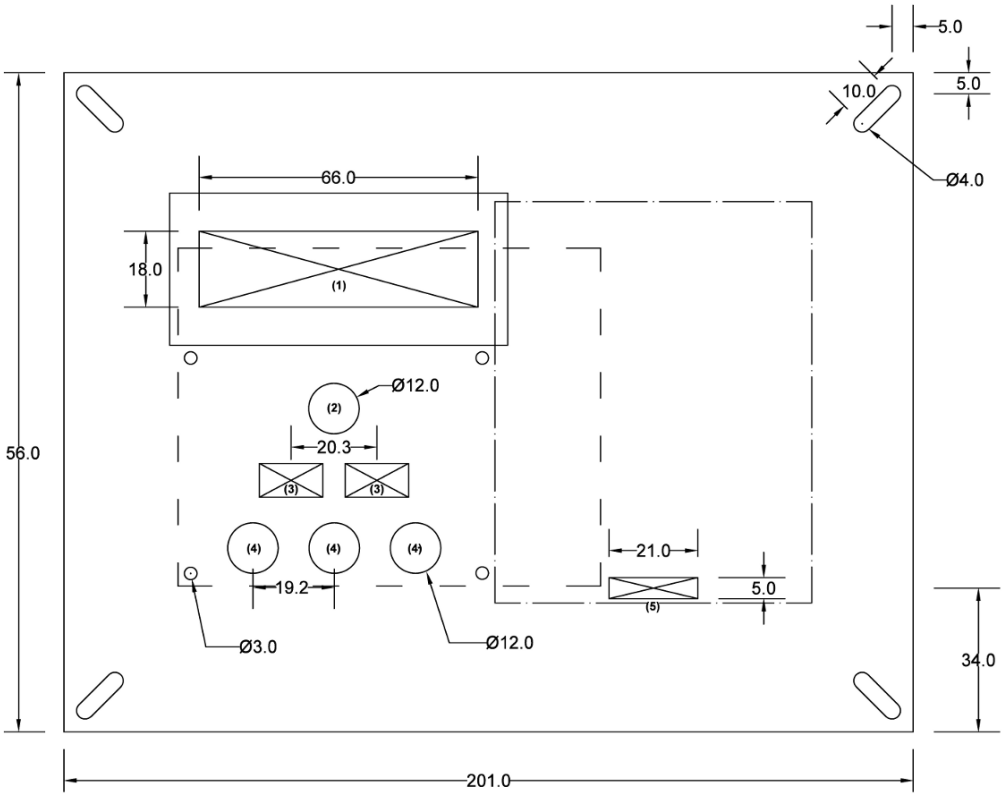


FIGURE 59 - INNER BOX DIMENSIONS WITH PCB, BOX, SCREEN AND KEYPAD LOCATIONS

## PCB

The PCB is designed to be produced by industrial pick and place machines which allows any organisation that use these designs to have the product manufactured by a third party. Component choices were made to ease this process, surface mount components are used wherever possible and non-standard parts were minimised. A simple, low density, two layer PCB design was produced which removes the need for expensive PCB manufacturing processes. All surface mount components have been kept on a single side of the PCB ensuring only a single pass through a pick and place machine is required and gluing is not needed, as shown in Figure 60. Passive component values have been agglomerated into as few values as possible which minimised the BOM. All of these techniques should aid in reducing the per unit assembly cost.

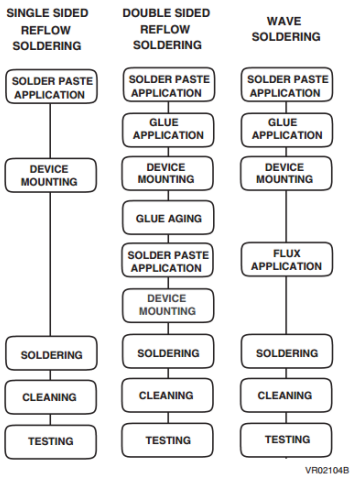


**FIGURE 60 – COMPARISON OF THE STEP REQUIRED FOR THREE DIFFERENT SOLDERING TECHNIQUES. THE NUMBER OF STEPS REQUIRED IS A GOOD INDICATION OF THE RELATIVE COST (39).**

One side of the PCB feature most of the electronic components in the design. The rear of the PCB is used for connectors which must be accesable from the faceplate, for example the USB sockets, DC Sockets and Power Switch. This results in an extremely simple to assemble final product but requires very careful component selection as all connectors must be of the correct height to mount flush with the faceplate. The device which determined the gap between the PCB and faceplate was the USB Socket as this is only available in one height. DC Sockets had to be compatible with the 2.5mm DC Jacks used on the LED Light's used by equinox and also needed to match the height of the USB Socket. These had to be sourced from a specialist connectors company in the UK.

The LCD must fit behind the faceplate and be directly soldered to the PCB. This component was sourced from a specialist LCD supplier based in China. There is enough space between the LCD screen and the faceplate for a protective clear plastic window which will protect the screen and prevent moisture and dirt entering the casing.

The switch was a difficult component to source as the switch must be matched with an appropriate cap to increase the radius of the switch presented to the user. Matching the cap, switch and dimensions required proved difficult but compatible devices were sourced from UK based suppliers. The switch cap is not physically attached to the PCB, rather it I mounted in the faceplate and held in place by the switch once the PCB is attached to the faceplate.

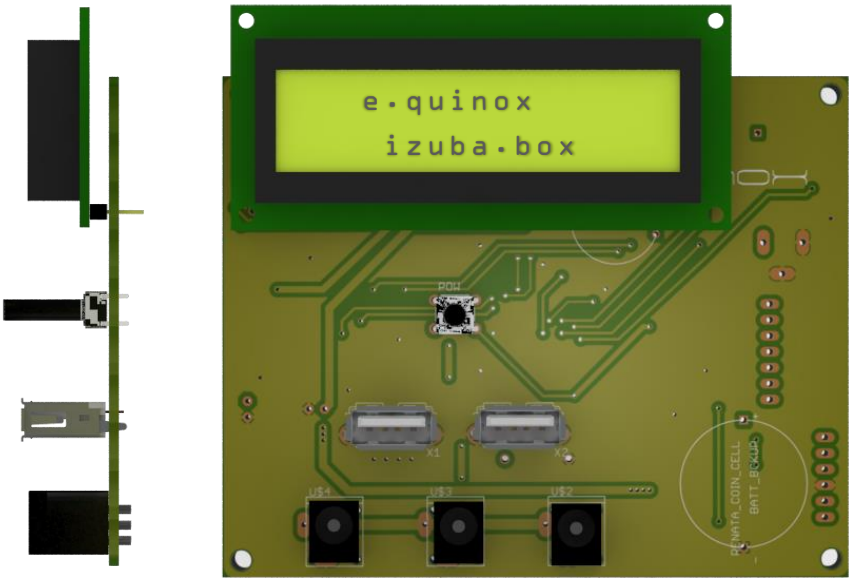


**Figure 61 – 3D Models of PCB and Components were used to Check Size and To Produce Design Renderings For Promotion of The Final Product. Note, Not all Electronic Components are Shown in this image for Clarity.**

E.quinox will be testing the automated assembly of these PCB for the products which will be distributed in summer 2013.

## PCB Layout

The PCB layout was determined predominantly by the design of the faceplate as the mounting holes and connectors must match. The input conditioning and measurement was placed as close as possible to the input connectors to reduce noise on the measurements. The charge controller DC-DC converter was also placed as close to the battery and PV panel connectors as possible to reduce the length of the power traces. The 5V DC-DC convertor was placed next to the USB outputs and the microcontroller was placed in the centre as it communicates with all sub-blocks of the system.

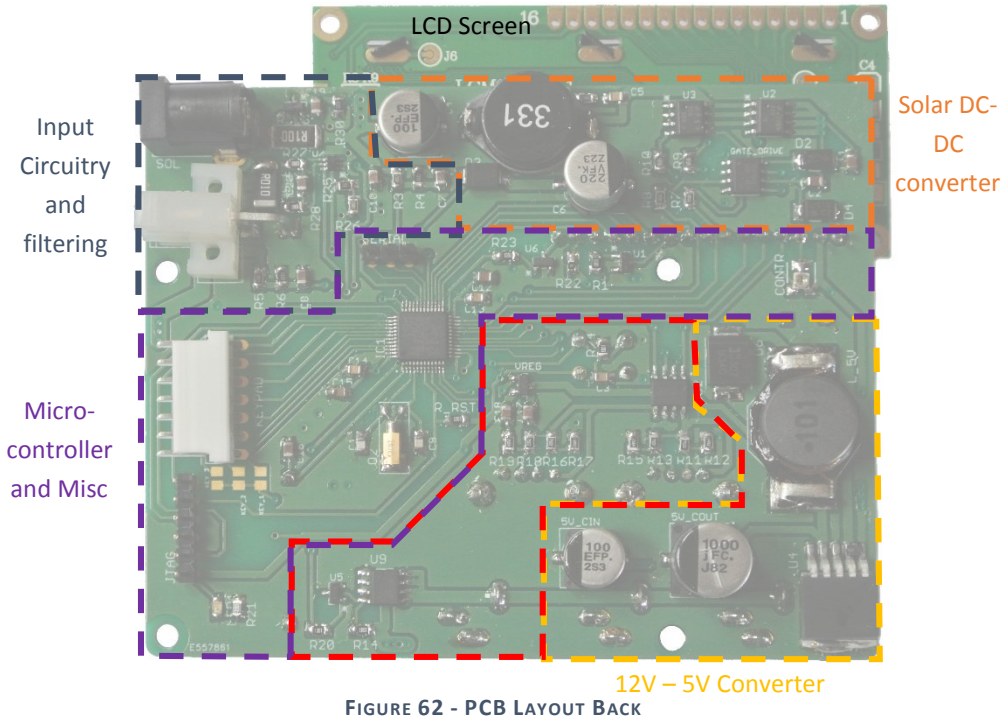


FIGURE 62 - PCB LAYOUT BACK

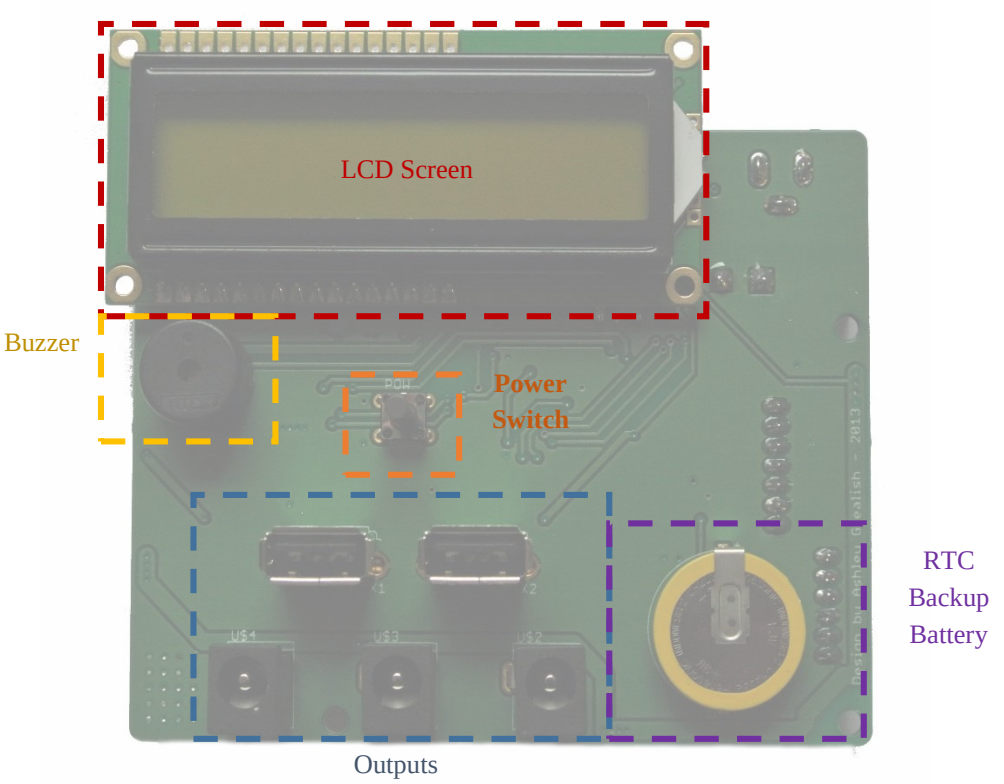


FIGURE 63 - PCB LAYOUT FRONT

# Future Work

## Long Term Battery Lifetime Analysis

The implemented charge controller was unable to go through long-term lifetime tests due to time constraints in this project. However, 100 units will be deployed in North Rwanda in summer 2013. Some of these units will be fitted with data-logging capabilities which will allow detailed analysis of battery lifetime in real use scenarios over a long time frame.

Due to time constraints a full data-logging system was not implemented, instead a serial port is broken out on the PCB which can be attached to third-party SD card logging systems such as the SDLogger (40). The serial port prints information such as battery and PV panel voltage and current, system state and temperature and can be used to plot data such as in Figure 47. These logging devices will only be fitted to a selection of these trial unit deployed in order to reduce cost. Combining data from these devices and customer feedback will allow a future e.quinox team to analyse the success of this project and properly analyse the suitability of this charge control algorithm.

In future versions of the product the on board microcontroller should be programmed to interact directly with a SD card. Minimal extra hardware would be required which will reduce the cost of the data-logging system which may, in future allow all units to log data.

## System Sizing

The product discussed in this report is an izuba.box home, which has a 12V 7Ah battery matched with a $7W_P$ PV Panel. e.quinox also has an izuba.box pro range which has a 26 Ah Battery, $35W_P$ PV Panel and more outputs including an AC output. The charge controller designed in this project was designed to work with panels up to 35 $W_P$ ensuring it is suitable for the pro unit. Little work is needed to convert the home design to a pro, mostly the work is simply added more output ports. 30 izuba.box pro units will be trialled in summer 2013.

The final product in the izuba.box range is the izuba.box mini. At this stage it is still a concept but plans to use a $1W_P$ PV Panel, 6V 1Ahr Ni-MH batteries and replace the expensive LCD with simpler LEDs. The charge controller hardware is suitable for this product but the software will need to be modified to suit Ni-MH batteries. The design and launch of the izuba.box mini will occur during 2014. This miniaturisation allows for an even cheaper price with a shorter pay-back period. This concept was derived from feedback from NGOs who currently distribute solar lanterns who felt that a two year payback period required too much financing and commitment.

**Figure 64 - Other izuba.box Models. The Smaller izuba.box mini on the left and the business customer focused izuba.box pro on the right. The hooks on the pro unit are designed to hold a DC-AC inverter.**

# Conclusion

This report has outlined the motivation behind the development of the izuba.box. This product alone cannot solve the massive and complex electrification problem but it does facilitate a financially viable business model which can be used to target the bottom-of-the pyramid customers. The monthly cost of the payment plan is designed to be less than customers were spending on low quality energy solution, so whilst this product may seem expensive at £62 it saves the end consumer money without the need for large up-front payments.

The most innovative part of the developed izuba.box is the intelligent charge controller which maximises battery lifetime. Research showed that Interrupted Charge Control (ICC) was the best candidate for optimising battery lifetime without compromising on the usability of the system. Research showed that the use of ICC could extend battery lifetime by 300-400% (41). This was combined with a maximum power point tracking algorithm called Perturb and Observe. The combination of these two technologies and intelligent temperature and charging current compensation is an innovative solution which should make the batteries used in solar systems last much longer. This firstly reduces system cost and has secondary benefits such as reducing the environmental impact of these products.

Full lifetime tests of the system were not possible during the timeframe of the project and temperature tests proved inconclusive. Future work is required to analyse the performance of the implemented battery lifetime optimisations. This has been facilitated by implementing optional data-logging support into the charge controller which can be used to analyse lifetime in real world applications.

The charge controller was integrated with a solar home system known as the izuba.box. The integration allowed the sharing of key system components such as the microcontroller and power supplies. The resulting system has greater intelligence and lower cost when compared with a system of discrete modules.

e.quinox aims to run a trial of 100 izuba.box units during the summer of 2013 and if successful, promote the concept and technical designs to larger organisations The izuba.box electronics and casing faceplate are open-source and designed to be suitable for machine assembly so that it can be easily duplicated by these larger organisations to begin to tackle the electrification problem. e.quinox has already received contact from several organisations who are interested in the project and who are considering trialling the system for themselves.

Work on this project will now be taken forward by non-graduating e.quinox members with aims to fix any issues that arise from the trial and analyse the real use performance of the battery lifetime optimisations. They also aim to use the developed system in a smaller, more affordable solar home system and well as a larger system aimed for small businesses. These are branded the izuba.box mini and izuba.box pro respectively.

Overall, this project has met its aims of producing a product which builds upon the successes of the 2012 prototype izuba.box and improves on its shortfalls It has resulted in a professional product that can be promoted to the wider development community as proof that a pay-as-you-go business model for rural electrification can help to target the bottom of the pyramid consumers.

# Bibliography

# BIBLIOGRAPHY


1. **World Bank.** Energy - The Facts. *World Bank.* [Online] World Bank, 2011. [Cited: 29 December 2012.] http://go.worldbank.org/6ITD8WA1A0.

2. **Lighting Africa.** In Numbers. *Lighting Africa.* [Online] Lighting Africa, 2012. [Cited: 29 December 2012.] http://www.lightingafrica.org/about-us/in-numbers.html.

3. **BTC.** Increased access to electricity for the rural population. *BTC.* [Online] BTC, 2009. [Cited: 29 December 2012.] http://www.btcctb.org/en/casestudy/increased-access-electricity-rural-population.

4. **International Finance Corporation.** *From Gap to Opportunity: Business Models for Scaling Up Energy Access.* s.l. : Iternational Finance Corporation, 2012.

5. **Prahalad, C. K.** *The Fortune at the Bottom of the Pyramid.* New York : Wharton School Publishing, 2005.

6. **Solar Sister.** What We Do. *Solar Sister.* [Online] Solar Sister, 2012. [Cited: 29 December 2012.] http://www.solarsister.org/what-we-do/.

7. **e.quinox.** About. *e.quinox.org.* [Online] e.quinox, 2012. [Cited: 22 December 2012.] http://e.quinox.org/index.php/about.

8. **Cleophas, Ahishakiye.** *e.quinox Impact.* [Facebook Message received on e.quinox page] London : s.n., 2012.

9. **IEC.** *61215.* s.l. : IEC, 1998.

10. **SunTech.** STP060S. *sunteech-power.com.* [Online] Aug 2007. http://www.solarenergyalliance.com/shop/solarpanels/pdf/STP060s-12Sb.pdf.

11. **ko4bb.com.** Solar Panel Optimizing Battery Charger. *ko4bb.com.* [Online] ko4bb.com, 18 April 2012. [Cited: 31 December 2012.] http://www.ko4bb.com/Solar_Optimizer/.

12. *Variable step size P&O MPPT algorithm for PV systems.* **Al-Diab, A.** s.l. : IEEE, 2010.

13. *Low cost MPPT controller for off grid solar applications.* **He, Zhongyi.** Shanghai : IEEE, 2012.

14. *Experimental test of seven widely-adopted.* **Berrera, M. and Dolara, A.** Milan : IEEE, 2009.

15. *Estimation of Global Solar Radiation in Rwanda Using Empirical Models.* **Safari, B. and Gasore, J.** s.l. : Asian Journal of Scientific Research, 2: 68-75, 2009, Vol. 2, pp. 68-75.

16. **Photovoltaic Solar Electricity Potential it the Mediterranean Basin, Africa and Southwest Asia.** ***http://soda-is.com/.*** **[Online] August 2008. [Cited: 24 May 2013.] http://soda-is.com/img/map_af_glob_opta_150dpi.png.**

**17. Grealish, Ashley. Solar Irradiation Data from Minazi, Northen Rwanda. 2012.**

**18. Battery University. What's the best Battery?** ***batteryuniversity.com.*** **[Online] batteryuniversity.com, 2013. http://batteryuniversity.com/learn/article/whats_the_best_battery.**

**19. Jenny, Chris. 5 Reasons Tesla Motors Will Thrive. *seekingalpha.com.* [Online] 21 Mar 2013. [Cited: 07 June 2013.] http://seekingalpha.com/article/1292591-5-reasons-tesla-motors-will-thrive.**

**20. Rand, D. A. J. *Valve-regulated Lead-acid Batteries.* s.l. : Elsevier Science Ltd, 2004.**

**21. *Evaluation of the Impact of the Different Charging Algorithms on the Lead-Acid Batteries Lifetime.* Yatsui, M. s.l. : IEEE, 2012.**

**22. *The effect of charge rate and depth of discharge on the cycle life of sealed lead-acid aircraft batteries.* Vutetakis, D.G. and Wu, H. s.l. : IEEE 35th International , vol., no., pp.103-105, 22-25 Jun 1992, 1992.**

**23. *Comparison of battery charging algorithms for stand alone photovoltaic systems.* Armstrong, S., Glavin, M.E. and Hurley, W.G. Rhodes : IEEE, 2008.**

**24. Farnell. STM32F050C6T6A . *Farnell.com.* [Online] [Cited: 09 June 2013.] http://onecall.farnell.com/stmicroelectronics/stm32f050c6t6a/mcu-32bit-arm-cortex-m0-48lqfp/dp/2115059.**

**25. ST. STM32F050x6 Datasheet. *st.com.* [Online] November 2012. [Cited: 09 June 2013.] http://www.st.com/st-web-ui/static/active/en/resource/technical/document/datasheet/DM00065136.pdf.**

**26. ARM. Keil MDK Solector. *Keil.* [Online] ARM. [Cited: 03 March 2013.] http://www.keil.com/arm/selector.asp.**

**27. Diodes Inc. farnell.com. *ZXCT1107 Datasheet.* [Online] March 2011. [Cited: 09 June 2013.] http://www.farnell.com/datasheets/1383710.pdf.**

**28. Texas Instruments. farnell.com. *INA213A.* [Online] 2009. [Cited: 09 June 2013.] http://www.farnell.com/datasheets/1633831.pdf.**

**29. ST. STM32F05xxx Reference manual. *st.com.* [Online] May 2013. http://www.st.com/web/en/resource/technical/document/reference_manual/DM00031936.pdf.**

**30. TI. Calculator for Buck Conveters. *ti.com.* [Online] TI. [Cited: 29 May 2013.] http://www.ti.com/tool/buck-convcalc.**

**31. *Temperature Compensation Algorithm for Interrupted Charge Control Regime for a VRLA Battery in Standby Applications.* Wong, Y.S. and Hurley, W.G. Galway : IEEE, 2008. 978-1-4244-1874-9/08/$25.00.**

**32. Yuasa. Yuasa NP Series. *farnell.com.* [Online] 2012. [Cited: 1 Janurary 2013.] http://www.farnell.com/datasheets/612553.pdf.**

**33. *Charge regimes for valve-regulated lead-acid batteries: Performance overview inclusive of temperature compensation.* Wong, Y.S., Hurley, W.G. and Wölfle, W.H. Galway : Journal of Power Sources, 2008, Vol. 183.**

**34. autonopedia.org/. Lead-Acid Battery State of Charge vs.Voltage. *autonopedia.org/.* [Online] autonopedia.org/, 2013. [Cited: 15 June 2013.] http://autonopedia.org/renewable-energy/energy-storage/soc-vs-volts/.**

**35. ladyada.net. Minty Boost.** ***ladyada.net.*** **[Online] 17 May 2011. http://www.ladyada.net/make/mintyboost/icharge.html.**

**36. —. Minty Boost Device Compatibility.** ***ladyada.net.*** **[Online] 17 May 2011. http://www.ladyada.net/make/mintyboost/compat3.html.**

**37. Panasonic. Precautions for handling valve regulated (sealed) lead-acid batteries.** ***industrial.panasonic.com.*** **[Online] [Cited: 10 June 2013.] http://industrial.panasonic.com/www-data/pdf/ACD4000/ACD4000PE7.pdf.**

**38. ST. EEPROM emulation in STM32F101xx and STM32F103xx microcontrollers.** ***st.com.*** **[Online] October 2007. [Cited: 12 June 2013.] http://www.st.com/web/en/resource/technical/document/application_note/CD00165693.pdf.**

**39. —. Soldering recommendations and package information for Lead-free ECOPACK microcontrollers.** ***st.com.*** **[Online] May 2013. [Cited: 09 June 2013.] http://www.st.com/st-web-ui/static/active/cn/resource/technical/document/application_note/CD00173820.pdf.**

**40. SeeedStudio. SDLogger - Open Hardware Data Logger.** ***seeedstudio.com.*** **[Online] [Cited: 03 June 2013.] http://www.seeedstudio.com/depot/sdlogger-open-hardware-data-logger-p-723.html.**

**41. NREL. Current Interrupt Charging Algorithm for Lead-Acid Batteries.** ***nrel.gov.*** **[Online] NREL, 2001. [Cited: 12 June 2013.] http://www.nrel.gov/awards/2001_current_interrupt.html?print.**

# Appendix

# HARDWARE DESIGNS

## SCHEMATICS

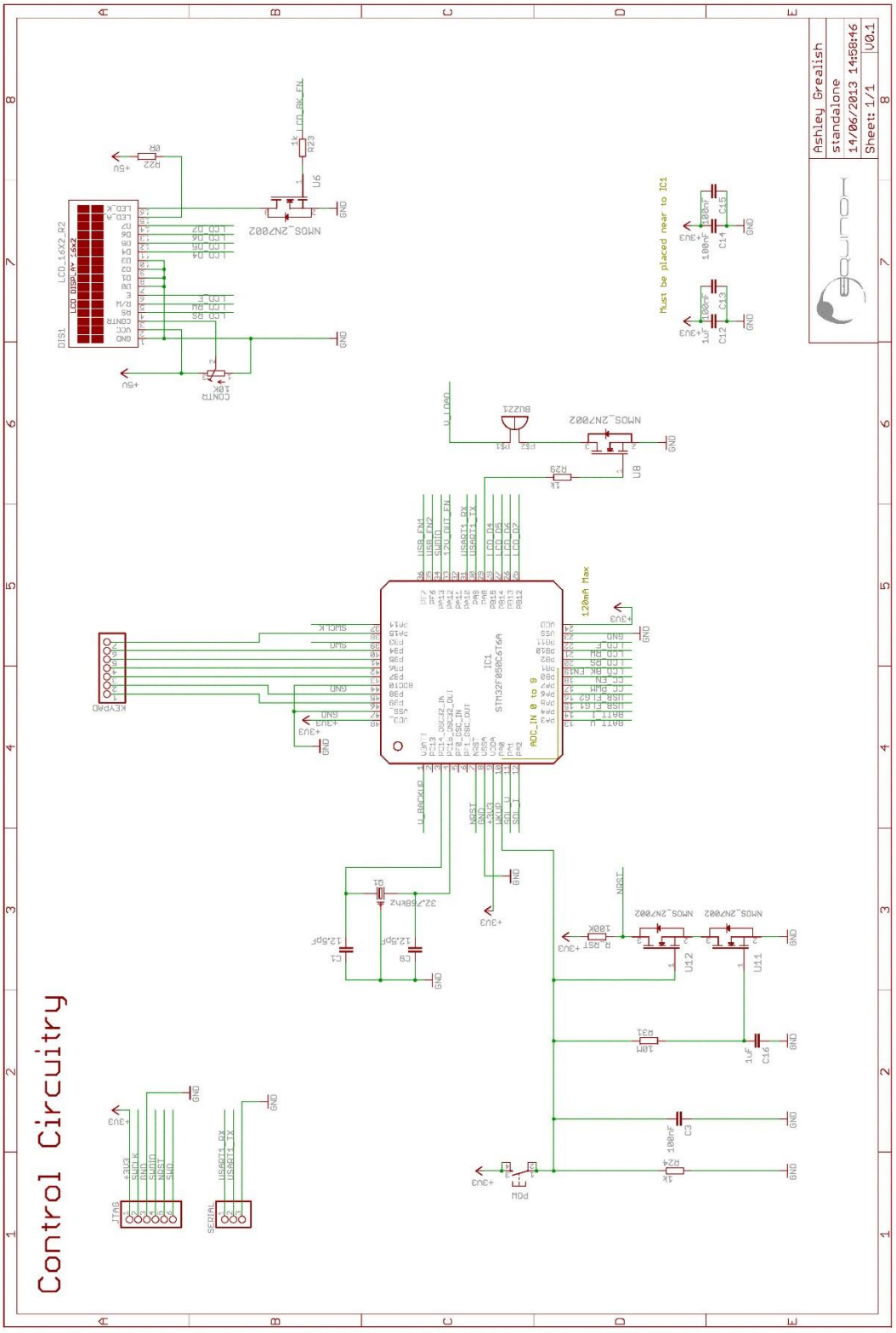

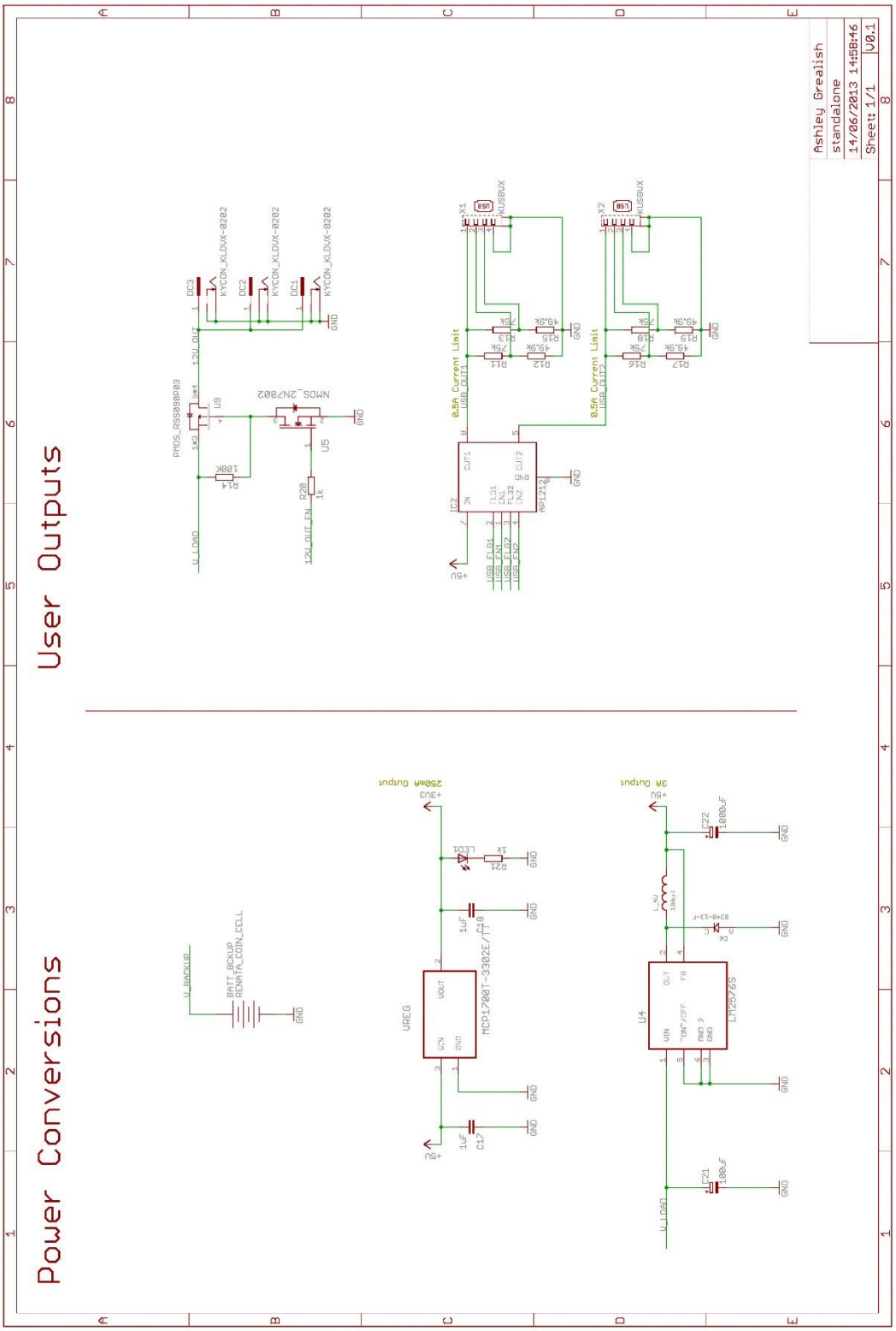
Power Conversions
User Outputs
Ashley Grealish
standalone
14/06/2013 14:58:46
Sheet: 1/1
V0.1
KYCON_KLDUX-0202
MOSFET_PMOS_RSS080P03
NMOS_2N7002
0.5A Current Limit
MCP1700T-3302E/TT
LM2576S
3A Output
250mA Output
BATT_BCKUP
RENATA_COIN_CELL

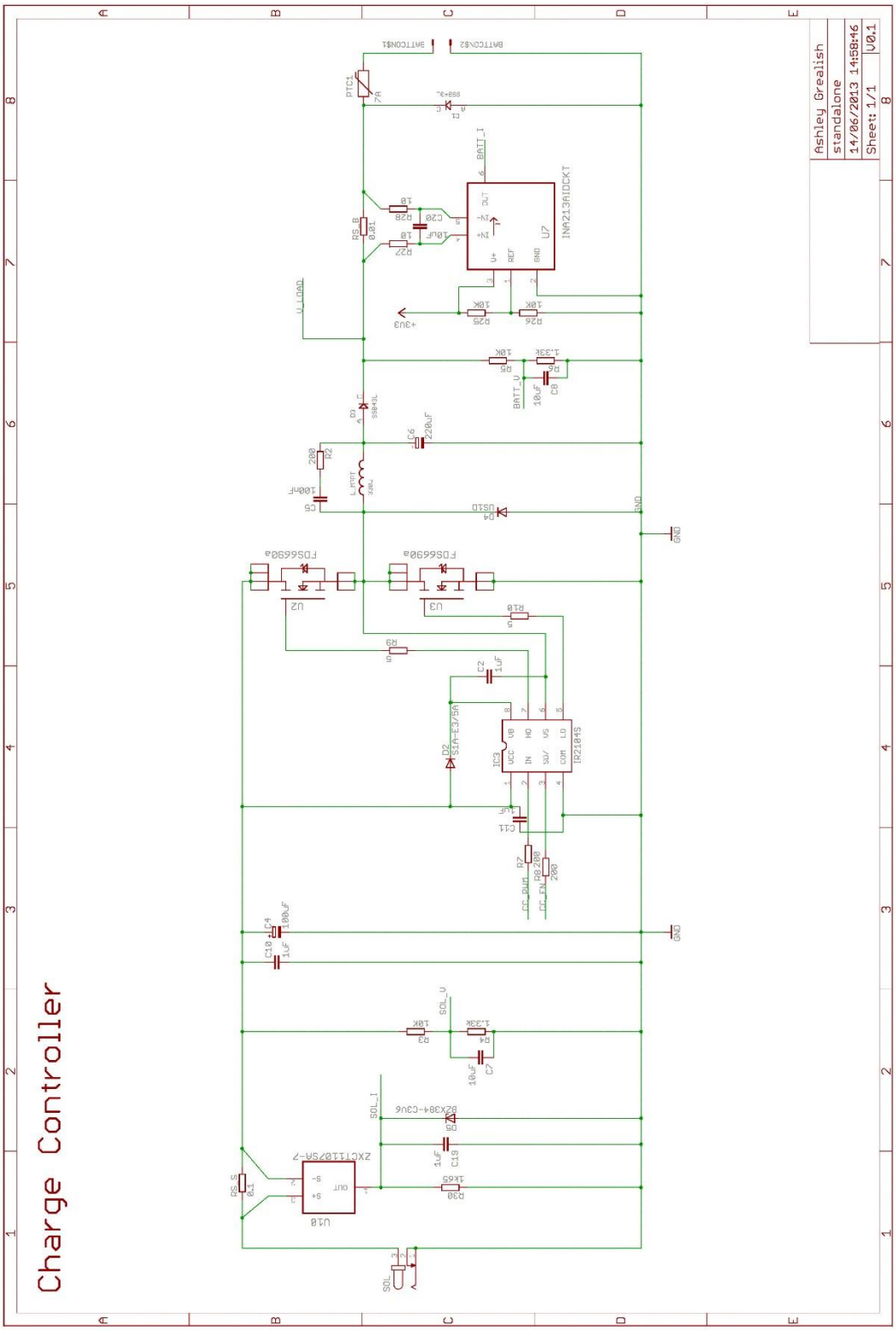
Charge Controller
Ashley Grealish
standalone
14/06/2013 14:58:46
Sheet: 1/1
V0.1
INA213A1DCKT
IR2104S
FDS6690a
ZXCT1107SA-7
BZX384-C3V6
GND
SOL
BATT_V
SOL_V
SOL_I
V_LOAD

## PCB Layout

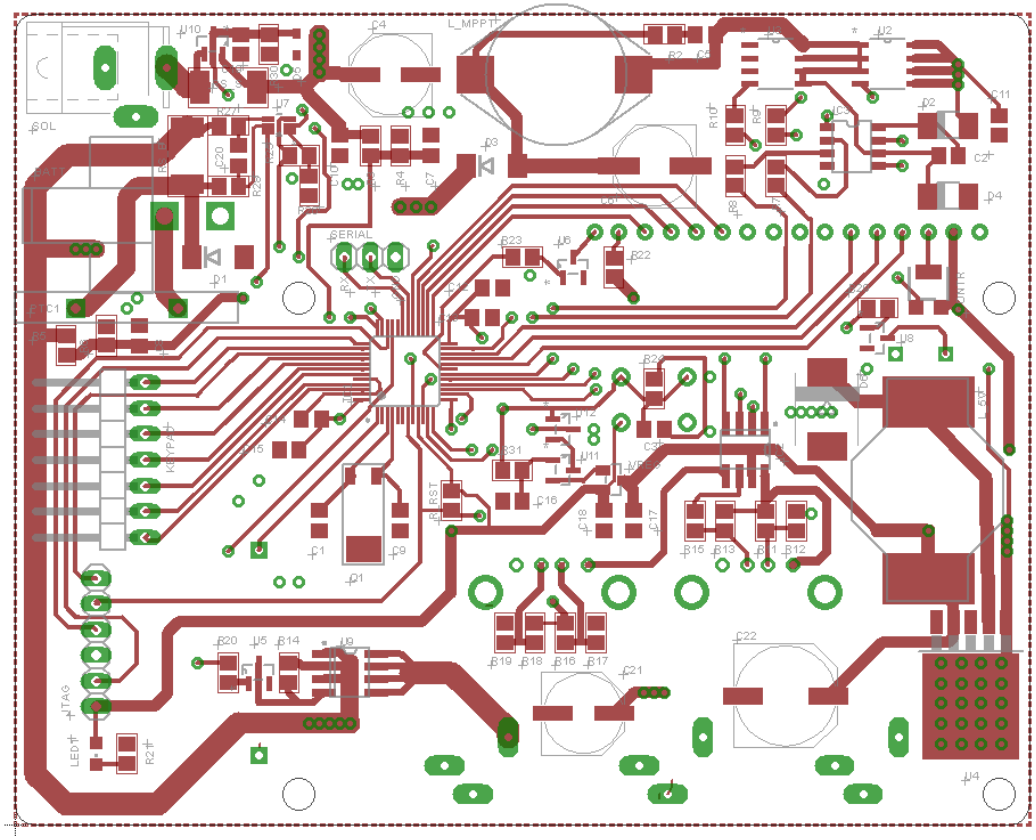

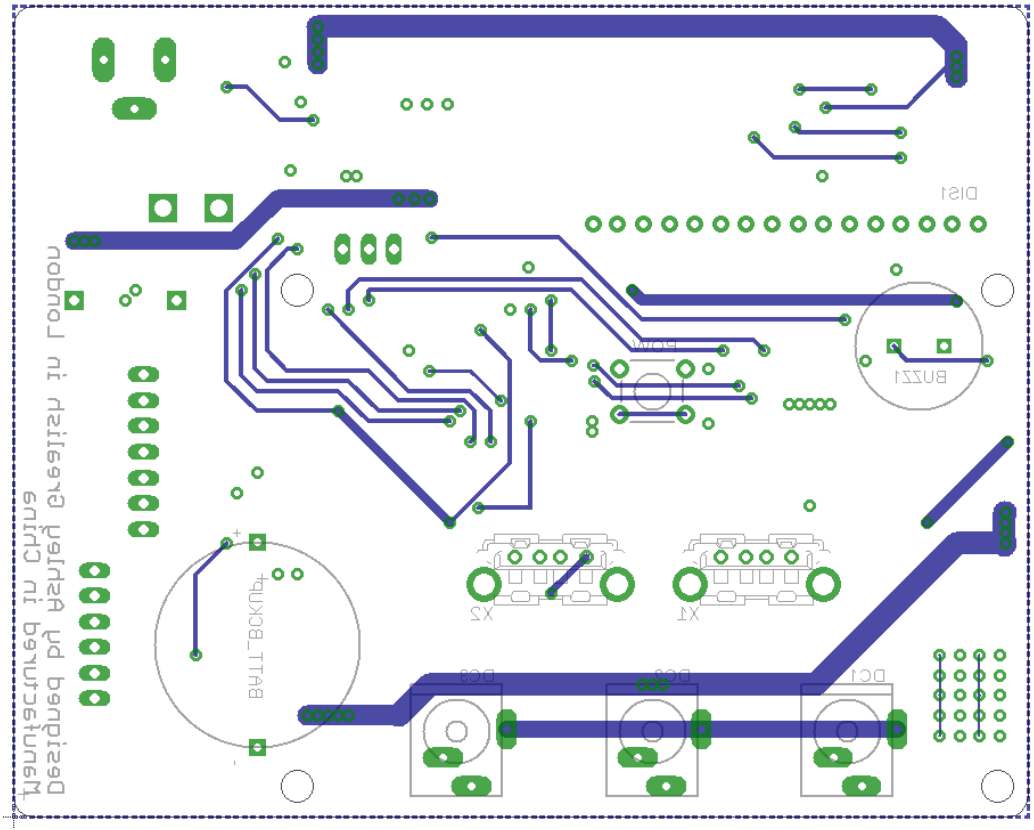
Designed by Aarya Creative in India
Manufactured in London

| Qty | Value | Populate | Device | Package | Parts | Description | OC_FARNELL | RS | TOBY | Price (Fc | Total Cost |
|---|---|---|---|---|---|---|---|---|---|---|---|
| 2 | 100uF | Y | CPOL-EUE | PANASONIC_E | 5V_CIN, C4 | POLARIZED CAPACITOR, European symbol | 1539489 | | | £ 0.17 | £ 0.34 |
| 1 | 1000uF | Y | CPOL-EUG | PANASONIC_G | 5V_COUT | POLARIZED CAPACITOR, European symbol | 1244342 | | | £ 0.34 | £ 0.34 |
| 1 | CON_MOLEX_39_29_1028 | Y | CON_MOLEX_39_29_1028 | MOLEX_39_29_1028 | BATT | | 1012166 | | | £ 0.29 | £ 0.29 |
| 1 | RENATA_COIN_CELL | Y | PANASONIC_CR2032_1298246 | PANASONIC_CR2032_1298246 | BATT_BCKUP | Farnell Part No: 1298246 | 1298246 | | | £ 0.76 | £ 0.76 |
| 1 | BUZZ_14MM | Y | BUZZ_14MM | 14MM_5M_PINS | BUZZ1 | | 1669967 | | | £ 0.16 | £ 0.16 |
| 2 | 12.5pF | Y | C-EUC0805K | C0805K | C1, C9 | CAPACITOR, European symbol | | | | £ 0.01 | £ 0.02 |
| 8 | 1uF | Y | C-EUC0805K | C0805K | C2, C10, C11, C12, C16, C17, C18, C19 | CAPACITOR, European symbol | | | | £ 0.01 | £ 0.08 |
| 5 | 100nF | Y | C-EUC0805K | C0805K | C3, C5, C13, C14, C15 | CAPACITOR, European symbol | | | | £ 0.01 | £ 0.05 |
| 1 | 220uF | Y | CPOL-EUF | PANASONIC_F | C6 | POLARIZED CAPACITOR, European symbol | 9695877 | | | £ 0.16 | £ 0.16 |
| 3 | 10uF | Y | C-EUC0805K | C0805K | C7, C8, C20 | CAPACITOR, European symbol | | | | £ 0.01 | £ 0.03 |
| 1 | 10K | Y | R-TRIMM3304W | RTRIM3304W | CONTR | Trimm resistor | | 725-0154 | | £ 0.11 | £ 0.11 |
| 1 | S1A-E3/5AT | Y | DIODE-DO-214AC | DO-214AC | D2 | DIODE | 9550216 | | | £ 0.05 | £ 0.05 |
| 1 | SSB43L | Y | DIODE_SSB43L | DO214AA | D3 | VISHAY - SSB43L-E3/52T - DIODE, SCHOTTKY, 4A, 30V | 1336556 | | | £ 0.22 | £ 0.22 |
| 1 | US1D | Y | DIODE-DO-214AC | DO-214AC | D4 | DIODE | 1625280 | | | £ 0.04 | £ 0.04 |
| 1 | B340-13-F | Y | DIODE_B340-13-F | SMC | D6 | | 1843695 | | | £ 0.10 | £ 0.10 |
| 1 | LCD_16X2_R2 | Y | LCD_16X2_R2 | LCD_16X2_R2 | DIS1 | Supplier: info@huaxinjin.com Order Code: HSM1602C-1 | | | | £ 1.17 | £ 1.17 |
| 1 | IR2104S | Y | IR2104S | IR2104S | GATE_DRIVE | Half Bridge Mosfet - IGBT driver SOIC | 8638756 | | | £ 0.85 | £ 0.85 |
| 1 | STM32F050C6T6A | Y | STM32F050C6T6A | LQFP48 | IC1 | | 2115059 | | | £ 1.24 | £ 1.24 |
| 1 | AP1212 | Y | AP1212 | SO8 | IC2 | Datasheet: http://www.farnell.com/datasheets/608 | 1825302 | | | £ 0.47 | £ 0.47 |
| 1 | | N | PINHD-1X6 | 1X06 | JTAG | PIN HEADER | | | | | £ - |
| 1 | | Y | PINHD-1X7/90 | 1X07/90 | KEYPAD | PIN HEADER | 588763 | | | £ 0.17 | £ 0.17 |
| 1 | 100uH | Y | INDUC_BOURNES_SDR2207 | INDUC_BOURNS_SDR2207 | L_5V | | 1612709 | | | £ 0.42 | £ 0.42 |
| 1 | 330u | Y | INDUC_BOURNES_SDR1806 | INDUC_BOURNS_SDR1806 | L_MPPT | Datasheet: http://www.bourns.com/data/global/pd | 1929706 | | | £ 0.40 | £ 0.40 |
| 1 | POW_3V3 | N | LEDCHIPLED_0805 | CHIPLED_0805 | LED1 | LED | | | | | £ - |
| 1 | | Y | TAC_SWITCHPTH | TACTILE-PTH | POW | Momentary Switch | | 758-1979 | | £ 0.20 | £ 0.20 |
| 1 | 32.768khz | Y | CRYSTAL_CMJ206T | CRYSTAL_CMJ206T | Q2 | Datasheet: http://cfm.citizen.co.jp/english/product/ | 2101358 | | | £ 0.21 | £ 0.21 |
| 5 | 1k | Y | R-EU_M0805 | M0805 | R1, R20, R21, R23, R24 | RESISTOR, European symbol | | | | £ 0.01 | £ 0.05 |
| 4 | 75k | Y | R-EU_M0805 | M0805 | R11, R13, R16, R18 | RESISTOR, European symbol | | | | £ 0.01 | £ 0.04 |
| 4 | 49.9k | Y | R-EU_M0805 | M0805 | R12, R15, R17, R19 | RESISTOR, European symbol | | | | £ 0.01 | £ 0.04 |
| 2 | 100K | Y | R-EU_M0805 | M0805 | R14, R_RST | RESISTOR, European symbol | | | | £ 0.01 | £ 0.02 |
| 3 | 200 | Y | R-EU_M0805 | M0805 | R2, R7, R8 | RESISTOR, European symbol | | | | £ 0.01 | £ 0.03 |
| 1 | 0R | Y | R-EU_M0805 | M0805 | R22 | RESISTOR, European symbol | | | | £ 0.01 | £ 0.01 |
| 2 | 10 | Y | R-EU_M0805 | M0805 | R27, R28 | RESISTOR, European symbol | | | | £ 0.01 | £ 0.02 |
| 4 | 10K | Y | R-EU_M0805 | M0805 | R3, R5, R25, R26 | RESISTOR, European symbol | | | | £ 0.01 | £ 0.04 |
| 1 | 1k65 | Y | R-EU_M0805 | M0805 | R30 | RESISTOR, European symbol | | | | £ 0.01 | £ 0.01 |
| 2 | 1.32k | Y | R-EU_M0805 | M0805 | R4, R6 | RESISTOR, European symbol | | | | £ 0.01 | £ 0.02 |
| 2 | 5 | Y | R-EU_M0805 | M0805 | R9, R10 | RESISTOR, European symbol | | | | £ 0.01 | £ 0.02 |
| 1 | 0.01 | Y | R-EU_R2512 | R2512 | RS_B | RESISTOR, European symbol | | | | £ 0.01 | £ 0.01 |
| 1 | 0.1 | Y | R-EU_R2512 | R2512 | RS_S | RESISTOR, European symbol | | | | £ 0.01 | £ 0.01 |
| 1 | | N | PINHD-1X3 | 1X03 | SERIAL | PIN HEADER | | | | | £ - |
| 1 | | Y | JACK-PLUG0 | SPC4077 | SOL | DC POWER JACK | unknown | | DC-001-A-2.1mm-R | £ 0.12 | £ 0.12 |
| 1 | EQUINOX_LOGO_LARGE | N | EQUINOX_LOGO_LARGE | EQUINOX_LOGO_LARGE | U$1 | | | | | | £ - |
| 3 | KYCON_KLDVX-0202 | Y | KYCON_KLDVX-0202 | KYCON_KLVDX_2020_B | U$2, U$3, U$4 | | | | DC-031-B | £ 0.25 | £ 0.75 |
| 3 | NMOS_2N7002 | Y | NMOS_2N7002 | SOT103P240X110-3N | U1, U5, U6 | N-CHANNEL ENHANCEMENT MODE FIELD EFFECT TRA | 1713823 | | | £ 0.06 | £ 0.17 |
| 1 | ZXCT1107SA-7 | Y | ZXCT1107SA-7 | SOT91P240X110-3N | U10 | LOW POWER HIGH-SIDE CURRENT MONITORS | 1904027 | | | £ 0.24 | £ 0.24 |
| 2 | FDS6690a | Y | DMS3016SSS-13 | SOIC127P600X175-8N | U2, U3 | ENHANCEMENT MODE MOSFET | 9845275 | | | £ 0.37 | £ 0.74 |
| 1 | LM2576S | Y | LM2576S | TO263-5 | U4 | | 1469178 | | | £ 1.23 | £ 1.23 |
| 1 | INA213AIDCKT | Y | INA213AIDCKT | SOT65P210X110-6N | U7 | CURRENT SHUNT MONITOR | 1754261 | | | £ 0.57 | £ 0.57 |
| 1 | PMOS_RSS090P03 | Y | PMOS_RSS090P03 | SO8 | U9 | | 1525544 | | | £ 0.25 | £ 0.25 |
| 1 | MCP1700T-3302E/TT | Y | MCP1700T-3302E/TT | SOT95P237X112-3N | VREG | Low Quiescent Current LDO | 1296592 | | | £ 0.16 | £ 0.16 |
| 2 | KUSBVX | Y | KUSBVX | KUSBVX | X1, X2 | Vertical,Top Entry Universal Serial Bus Connector KU | 2112372 | | | £ 0.12 | £ 0.24 |
| | | | | | | | | | | | |
| | | | | | | | | | | | **£ 12.66** |

## Software Designs

Full software listings are not included here but are downloadable at:
https://github.com/equinoxorg/standalone_v2/tree/master/Software

# MECHANICAL DESIGNS



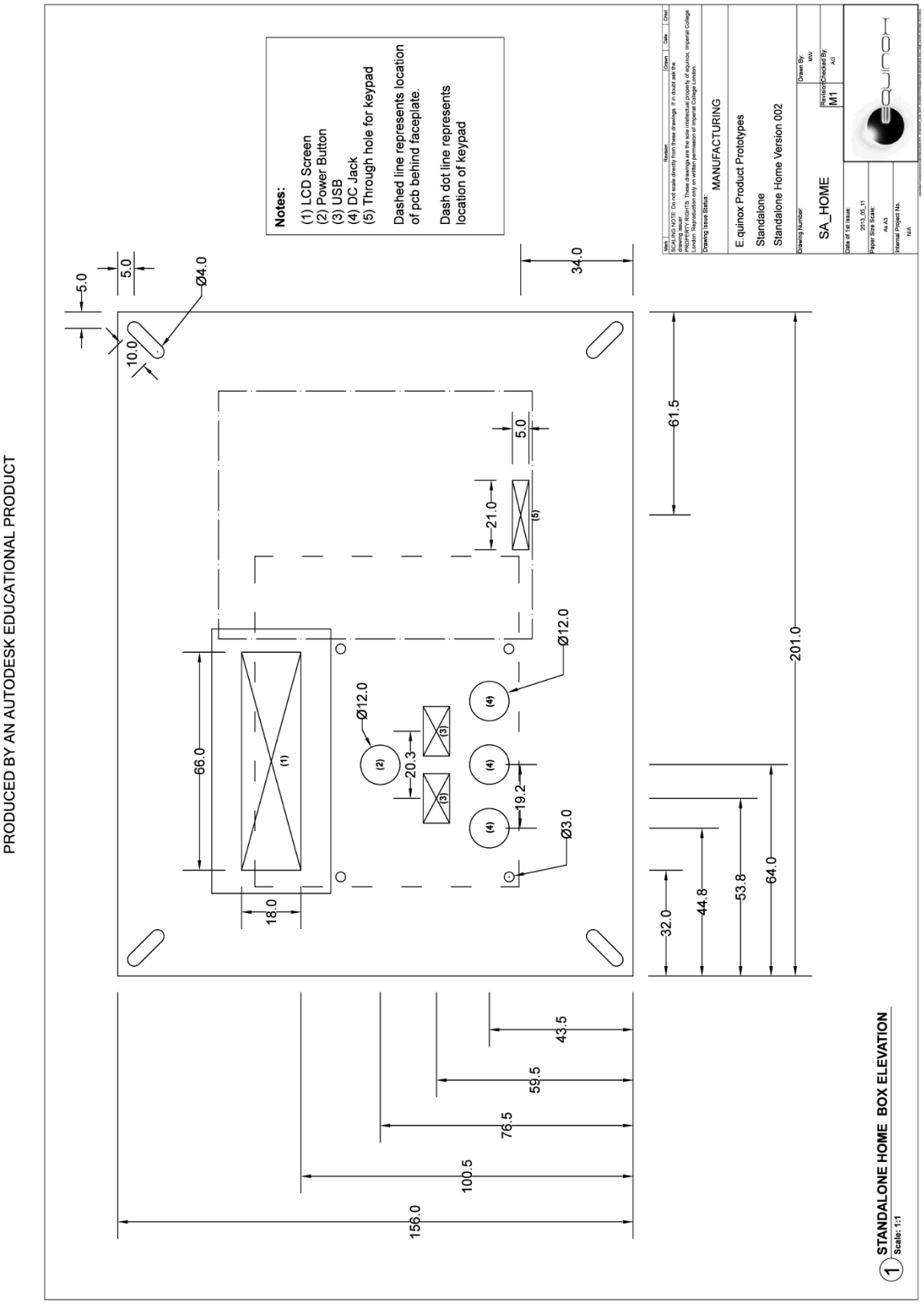




PRODUCED BY AN AUTODESK EDUCATIONAL PRODUCT